

AD-759 541

ENERGY SPECTRA OF THE OCEAN SURFACE:
AN EIGENMODE APPROACH

Kenneth M. Watson, et al

Physical Dynamics, Incorporated

Prepared for:

Rome Air Development Center
Defense Advanced Research Projects Agency

February 1973

DISTRIBUTED BY:

NTIS

National Technical Information Service
U. S. DEPARTMENT OF COMMERCE
5285 Port Royal Road, Springfield Va. 22151

RADC-TR- 73-74
Technical Report
February 1973



ENERGY SPECTRA OF THE OCEAN SURFACE:
AN EIGENMODE APPROACH

Physical Dynamics, Inc.

Sponsored by
Defense Advanced Research Projects Agency
ARPA Order No. 1649

Approved for public release;
distribution unlimited.

The views and conclusions contained in this document are those of the authors and should not be interpreted as necessarily representing the official policies, either expressed or implied, of the Defense Advanced Research Projects Agency or the U. S. Government.

Reproduced by
NATIONAL TECHNICAL
INFORMATION SERVICE
U S Department of Commerce
Springfield VA 22151

Rome Air Development Center
Air Force Systems Command
Griffiss Air Force Base, New York



AD 759541

UNCLASSIFIED

Security Classification

DOCUMENT CONTROL DATA - R & D		
(Security classification of title, body of abstract and indexing annotation must be entered when the overall report is classified)		
1. ORIGINATING ACTIVITY (Corporate author) Physical Dynamics, Inc. P.O. Box 1069 Berkeley, Calif. 94701		2a. REPORT SECURITY CLASSIFICATION UNCLASSIFIED
		2b. GROUP
3. REPORT TITLE ENERGY SPECTRA OF THE OCEAN SURFACE: AN EIGENMODE APPROACH		
4. DESCRIPTIVE NOTES (Type of report and inclusive dates) Scientific Report		
5. AUTHOR(S) (First name, middle initial, last name) Kenneth M. Watson, Bruce J. West, J. Alex Thomson		
6. REPORT DATE February 1973	7a. TOTAL NO. OF PAGES 72	7b. NO. OF REFS 7
8a. CONTRACT OR GRANT NO. F30602-72-C-0494	9a. ORIGINATOR'S REPORT NUMBER(S) PD 72-030	
b. PROJECT NO. 16490402		
c. Program Code No. 2E20	9b. OTHER REPORT NO(S) (Any other numbers that may be assigned this report) RADC-TR-73-74	
d. ARPA Order 1649		
10. DISTRIBUTION STATEMENT Approved for public release; distribution unlimited.		
11. SUPPLEMENTARY NOTES Monitored by: Leonard Strauss (RADC/OSCE) Griffiss AFB, N.Y. 13441 (315)-330-3055		12. SPONSORING MILITARY ACTIVITY Defense Advanced Research Projects Agency 1400 Wilson Blvd. Arlington, Va. 22209
13. ABSTRACT A set of Hermitian equations is constructed using a mode description of the dynamic equations of the ocean surface. These equations are sufficiently flexible to include the coupling of the ocean surface to the wind, viscous damping and the effects of surface tension as well as the non-linear interactions between surface waves. The system of equations is exact and from them a system of approximate, first-order (in time), finite differential equations is derived and solved numerically. The solutions to these coupled equations provide one with a detailed view of the growth of the non-linear surface waves and energy spectrum with time.		

DD FORM 1 NOV 65 1473

UNCLASSIFIED

Security Classification

ENERGY SPECTRA OF THE OCEAN SURFACE:
AN EIGENMODE APPROACH

Kenneth M. Watson
Bruce J. West
J. Alex Thomson

Contractor: Physical Dynamics, Incorporated
Contract Number: F30602-72-C-0494
Effective Date of Contract: 1 May 1972
Contract Expiration Date: 30 April 1973
Amount of Contract: \$48,118.00
Program Code Number: 2E20

Principal Investigator: J. Alex Thomson
Phone: 415-848-3063
Project Engineer: Joseph J. Simons
Phone: 315-330-3055
Contract Engineer: Leonard Strauss
Phone: 315-330-3055

Approved for public release;
distribution unlimited.

This research was supported by the
Defense Advanced Research Projects
Agency of the Department of Defense
and was monitored by Leonard Strauss,
RADC(OCSE), GAFB, NY 13441 under
Contract F30602-72-C-0494.

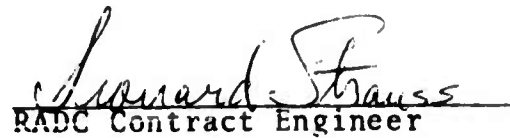


il

PUBLICATION REVIEW

This technical report has been reviewed and is approved


RADC Project Engineer


RADC Contract Engineer

ABSTRACT

A set of Hermitian equations is constructed using a mode description of the dynamic equations of the ocean surface. These equations are sufficiently flexible to include the coupling of the ocean surface to the wind, viscous damping and the effects of surface tension as well as the non-linear interactions between surface waves. The system of equations is exact and from them a system of approximate, first-order (in time), finite differential equations is derived and solved numerically. The solutions to these coupled equations provide one with a detailed view of the growth of the non-linear surface waves and energy spectrum with time.

ACKNOWLEDGMENTS

The authors would like to thank S. Singer and B. Cohen for their development of the computer code and calculations made thereon.

TABLE OF CONTENTS

	page
ABSTRACT	iii
ACKNOWLEDGMENTS	iii
LIST OF FIGURES	vii
1. INTRODUCTION	1
2. MODE COUPLING ANALYSIS	7
3. EIGENMODE DESCRIPTION	17
3A. The Approximate Equations	22
3B. The Resonance Condition	26
4. DISCUSSION OF EQUATION (3.29)	31
5. SEA SURFACE CONTOUR AND ENERGY	39
6. SAMPLE CALCULATION AND CONCLUSION	43
APPENDIX A	61
REFERENCES	65

LIST OF FIGURES

	<u>page</u>
1. The minimum ratio of the frequency mismatch to the primary frequency vs. the ratio of the off resonance wave numbers [Equation (4.7)].	34
2. The relative strength of the coupling coefficient $(-\Gamma_{nk}/\omega_k)$ as a function of the relative size of the wavenumber (k/n) .	36
3. The energy distribution between the 9 mode slopes at 4 different times. The central mode is $k = 0.02863 \text{ cm}^{-1}$ and the step size (Δk) is 0.2863 cm^{-1} .	46
4. The energy distribution between the 13 mode slopes at 4 different times. The central mode and step size are the same as in Figure 3.	47
5. The growth of the energy in the 9 mode test calculation given as a continuous function of time. The secondary modes are compared to a Born approximation calculation of their growth.	48
6. The envelope of the surface waves for 3 different times. The significant structure lies between the bumps situated at $x=0$ and $x=100 \lambda_p$.	51
7. The distortion of the surface envelope plotted as a function of time for the 9 mode test calculation and the simulated Benjamin-Feir experiment.	54

	<u>page</u>
8. The energy distribution between the 9 mode slopes for the simulated B-F experiment at 5 different times. The centered mode is $k = 0.02863 \text{ cm}^{-1}$ and the step size (Δk) is 0.2863 cm^{-1} .	55
9. The energy distribution between the 13 mode slopes for the simulated B-F experiment at 4 different times. The centered mode is $k = 0.02863 \text{ cm}^{-1}$. and the step size (Δk) is 0.14365 cm^{-1} .	57
10. The envelope of the surface waves depicted for three different times, comparing the 9 and 13 mode simulations of the B-F experiment. The amplitude scale is arbitrary since the two curves have been displaced to aid in the visual comparison.	58

ENERGY SPECTRA OF THE OCEAN SURFACE:
AN EIGENMODE APPROACH

by

Kenneth M. Watson
Bruce J. West
J. Alex Thomson

1. INTRODUCTION

The problem we wish to discuss in this report is how to describe the physical structure of the ocean's surface by means of a direct calculation of the non-linear interactions between gravity waves. Some of the interactive mechanisms themselves had not been identified until the last decade; so it is no surprise that there does not exist as yet a cohesive theory which presumes to calculate the surface structure of the ocean from first principles. The extreme difficulty of the problem lies in the nonlinear character of the interaction process which necessitates the construction and solution of non-linear models.

Theoretical models describing the ocean surface and the interaction of surface waves with surface waves, and surface waves with internal waves, fall into two rather broad categories. The first category comes under the general heading of Ray Theory, which is space oriented and primarily concerned with wave packets, e.g., Whitham (1966). In this type of theory one has position and time dependent wavenumbers and frequencies. The wave packet models are also known

as WKB or eikonal theories. They consider the ocean surface as essentially a superposition of a number of spatially localized wave packets, each distinguished by a characteristic wavenumber k and frequency ω which are related by means of a dispersion relation. These wave packets move along trajectories defined by the wave conservation equations

$$\frac{d\vec{x}}{dt} = \nabla_{\vec{k}} \omega \quad (1.1)$$

and

$$\frac{d\vec{k}}{dt} = -\nabla_{\vec{x}} \omega \quad (1.2)$$

which defines the paths along which energy naturally propagates.

The second approach and the one we will use in this paper is a modal description of the interaction process. The mode oriented models describe the ocean surface as a superposition of waves (in the unperturbed ocean this would be a superposition of sine waves). Such models generally concentrate their attention on the transfer of energy between the different modes. The most complete theory using such a method is that due to Hasselman (1961). He introduces the mode expansion for the surface elevation and velocity potential in the dynamic equation for the ocean surface, as is shown in Section 2. In addition, each mode is expanded in a perturbation series using the slope of the waves as a smallness parameter. The non-linear interactions are given at each order in perturbation theory by the product of an appropriate number of first order terms. By

assuming that the sea state is initially Gaussian, an expression for the redistribution of energy between the interacting modes is obtained.

In a later paper (1966), Hasselman structures the modal problem so as to make applicable the methods of Field Theory. The non-linear interactions enter this structure as perturbation diagrams of increasing order, just as in Quantum Field Theory and Nuclear Physics. However, all the difficulties of convergence and mathematical opacity also attend this approach, making practical calculations without the assumption as to the statistical nature of the sea state uncertain.

In the limiting case of small amplitude waves, both treatments, i.e., rays and modes, are equivalent since the requirements for validity of the WKB approximation are usually well satisfied for the waves of interest. This equivalence is often obscured in the development of models since spatial structure is bound up in the details of the phase relationship between different wavenumbers in a mode description; whereas the wavenumber structure is dependent on the details of the spatial correlations function in the wave packet description.

In Section 2 our model ocean is defined in terms of Bernoulli's equation for the ocean surface and the kinematic boundary condition at that surface. In a mode description these equations are reduced to a set of coupled equations which have

only first order derivatives in time. The method of keeping the first order simplicity of the equations is to introduce a set of hermitian variables. These variables essentially decouple the equations into a set of right and left moving waves, with the amplitudes $q_k^{(+)}$ and $q_k^{(-)}$, respectively. The rapid time oscillating part of the mode (Fourier) amplitudes for the velocity potential (ϕ_k) and surface elevation (ζ_k) is in this way removed so that $q_k^{(+)}$ and $q_k^{(-)}$ are slowly varying functions of time. These new mode amplitudes refer to a Fourier expansion in both space and time.

The utility of such a representation of the surface elevation and velocity potential is explored in Section 3, where the original coupled equations are cast in the form of an uncoupled eigenmode equation. In this representation the only variation in the $q_k^{(\pm)}$ amplitudes comes directly from the nonlinear interactions which are in terms of multiple products of these amplitudes. For calculational expediency the exact equations are expanded and the terms grouped so as to give second, third and higher order interactions. The expansion parameter is again a wave slope, but we expand only exponential terms and do not use perturbation theory. This we feel obviates some of the difficulty encountered in Hasselman's treatment of the problem.

In Section 3B the specialized problem of the interaction of only surface gravity waves is discussed. A resonance (frequency matching) condition simplifies the eigenmode equations so that only the third order interaction terms contribute to the rate equations for the system. A discussion of the integration procedure to be used in obtaining the numerical solution to the problem is presented in the appendix. The integration technique employed allows one to take large time steps on a scale corresponding to the oscillating part of the solution. This is done by integrating the rapidly oscillating part of the interaction coefficient analytically and numerically integrating only the slowly varying part. This technique was used successfully [Cohen, et al (1971)] in the treatment of the laser heating of plasmas.

Section 4 explores some of the specialized types of interaction, such as self-interaction and the scattering of waves which do not change in wavenumber. The connection with the nonlinear Stokes wave is also made here. The form of the surface contours and the representation of the sea spectrum in terms of the $q_k^{(\pm)}$ - amplitudes is discussed in Section 5.

A preliminary calculation is presented in Section 6, which has direct bearing on the experiment of Benjamin and Feir (1967) in which they determined a single gravity wave to be unstable. A single mode of large amplitude is allowed to interact with

its side bands which are an order of magnitude smaller in amplitude. It is observed in the calculation that energy diffuses out of the primary mode into the other modes in the system, until the neighboring and primary modes are of comparable amplitude. Energy is then transferred rapidly between all the modes in this region of k -space. The spatial picture of the surface when this rapid transfer process takes place is a breakup of the primary wave into a number of wave packets. This breakup into packets is the instability found by Benjamin and Feir. A detailed comparison with these results is made in the text.

2. MODE COUPLING ANALYSIS

In the following analysis, the ocean is assumed to be homogeneous and irrotational, that is, if ϕ is the potential describing the velocity field ($\vec{u} = \nabla\phi$), then $\nabla \times \vec{u} = 0$. The velocity potential also satisfies Laplace's equation

$$\nabla^2 \phi = 0 , \quad (2.1)$$

since the fluid is assumed to be incompressible. If we define the quantities: ρ as the fluid density, \vec{g} as the gravitational acceleration, and p as the pressure, we may write the momentum equation of the fluid as

$$\frac{d\vec{u}}{dt} = - \frac{1}{\rho} \Delta p + \vec{g} . \quad (2.2)$$

In terms of the velocity potential, Equations (2.2) may be written as,

$$\frac{d\vec{u}}{dt} = \nabla \left[\frac{\partial \phi}{\partial t} + \frac{1}{2} \nabla \phi \cdot \nabla \phi \right] = -\nabla \left\{ \frac{p}{\rho} + gz \right\} \quad (2.3)$$

where we have made use of the fact that the d/dt is the Eulerian derivative

$$\frac{d}{dt} = \frac{\partial}{\partial t} + \nabla \phi \cdot \nabla , \quad (2.4)$$

the density ρ is constant (assumed) and z is the vertical coordinate.

We may integrate Equation (2.3) immediately to obtain

$$\phi_t + \frac{1}{2} \nabla \phi \cdot \nabla \phi + \frac{\Delta p}{\rho} + g z = 0 \quad \text{at } z = \zeta \quad (2.5)$$

with the condition that hydrostatic equilibrium must prevail at infinity, where Δp is the incremental pressure with respect to ambient and $z = \zeta$ is the free surface of the ocean. A second equation may be obtained by recalling that the rate of increase in the wave height following a fluid element is the vertical component of the fluid velocity:

$$\frac{d\zeta}{dt} = \frac{\partial \phi}{\partial z} \quad \text{at } z = \zeta \quad (2.6)$$

Using the notation $(\tilde{\nabla})$ for the horizontal gradient, we may write Eq. (2.5) and (2.6) as

$$\phi_t + \frac{1}{2} (\nabla \phi)^2 + g \zeta + \Delta p / \rho = 0 \quad \text{at } z = \zeta \quad (2.7a)$$

and

$$\zeta_t + \tilde{\nabla} \phi \cdot \tilde{\nabla} \zeta - \phi_z = 0 \quad \text{at } z = \zeta, \quad (2.7b)$$

as the set of coupled equations describing the ocean surface.

To obtain an expression for the pressure in Eq. (2.7a), we must consider the fact that the interface between two fluids is in a state of uniform tension. The pressure condition at this interface can be obtained by considering the vertical forces acting on a strip of surface of width δx . If p is the pressure just below the water surface, p_a the pressure of the

air and T_1 the surface tension, then

$$(p - p_a) \delta x + \delta \left[T_1 \frac{\partial \zeta}{\partial x} \right] = 0 \quad (2.8)$$

is the force balance acting on the strip δx . We therefore have

$$p = p_a - T_1 \frac{\partial^2 \zeta}{\partial x^2} \quad (2.9)$$

The quantity p_a is variable if there is a wind blowing over the ocean surface. We model this variation in pressure by the expression

$$\frac{1}{\rho} p_a = \alpha \frac{\partial \zeta}{\partial x} + p_{\text{ambient}} \quad (2.10)$$

which gives the in-phase pressure variation at the surface due to the action of the wind.* Substituting Eqs. (2.9) and (2.10) into (2.7a) yields

$$\phi_t + \frac{1}{2} (\nabla \phi)^2 + g\zeta + \alpha \frac{\partial \zeta}{\partial x} - \gamma \frac{\partial^2 \zeta}{\partial x^2} = 0 \quad (2.11)$$

where we have assumed conditions to be completely uniform in the y-direction, i.e., a series of ridges.

In the above equations (2.11) and (2.7b), we have assumed the existence of a velocity potential ($\vec{u} = \nabla \phi$) based on the assumption that the ocean is irrotational. We have also pro-

* Equation (2.10) is intended to indicate how one includes the contribution from the wind in the dynamic equations, the detailed form of the term will change in a realistic calculation, e.g., making α a function of k as in the Miles-Phillips Model.

vided a means by which energy is supplied to the surface waves, i.e., by the action of the wind. We must now discuss the mechanisms by which this energy supplied by the wind may be dissipated. The most dramatic process is the formation of "white caps" or wave breaking. In our model this breaking directly transfers energy into heat and therefore out of the wave system and is not directly included in the above equations. The "white capping" should appear as instabilities in the above solutions when the wave slope has exceeded some critical value. A second mechanism for the dissipation of energy is the action of molecular viscosity, which has not as yet been included in the above equations.

To model the effect of viscosity, we first transform the system into a modal description by introducing the plane waves

$$\chi_k(x) = e^{ikx}/\sqrt{L} \quad (2.12)$$

where L (= length) is a dimension of interest for the problem, and decompose the vector potential and wave amplitude into their Fourier components,

$$\phi(x, z, t) = \sum_k \chi_k(x) e^{|k|z} \phi_k(t) \quad (2.13)$$

and

$$\zeta(x, t) = \sum_k \chi_k(x) \zeta_k(t) \quad (2.14)$$

Introducing Eqs. (2.13) and (2.14) into Eqs. (2.11) and (2.7b) yields the set of coupled equations in terms of the modal amplitudes,

$$\sum_k \chi_k(x) \left\{ \dot{\phi}_k e^{|k|z} + g\zeta_k + iak\zeta_k + \gamma k^2 \zeta_k \right\} = -\frac{1}{2} (\nabla\Phi)^2; \quad z = \zeta \quad (2.15)$$

and

$$\sum_k \chi_k(x) \left\{ \zeta_k - |k|\phi_k e^{|k|z} \right\} = -\tilde{\nabla}\Phi \cdot \tilde{\nabla}\zeta; \quad z = \zeta \quad (2.16)$$

We wish to rewrite Eqs. (2.15) and (2.16) in a form where the left hand sides of the equations are linear and the right hand sides contain all the non-linear coupling effects. To do this we evaluate $(\nabla\Phi)^2$ and $\tilde{\nabla}\Phi \cdot \tilde{\nabla}\zeta$ to be as follows:

$$\begin{aligned} (\nabla\Phi)^2 &= \phi_x^2 + \phi_z^2 \\ &= - \sum_{\ell, p} (\ell p - |\ell||p|) \phi_\ell \phi_p e^{(|\ell|+|p|)z} \chi_\ell \chi_p \end{aligned} \quad (2.17)$$

and

$$\tilde{\nabla}\Phi \cdot \tilde{\nabla}\zeta = - \sum_{\ell, p} \ell p \phi_\ell \zeta_p e^{|\ell|z} \chi_\ell \chi_p \quad (2.18)$$

and remove the exponentials to the right hand side of Equations (2.15) and (2.16). Then by multiplying these equations by $\chi_k^*(x)$ and integrating over x , we obtain

$$\begin{aligned}
\dot{\phi}_k + g\zeta_k &= \frac{1}{2} \sum_{\ell, p} (\ell p - |\ell||p|) \phi_\ell \phi_p \\
&\quad \int e^{(|\ell|+|p|)\zeta(x)} \chi_\ell(x) \chi_p(x) \chi_k^*(x) dx \\
&\quad - \sum_{\ell} \dot{\phi}_\ell \int (e^{|\ell|\zeta(x)} - 1) \chi_\ell(x) \chi_k^*(x) dx \\
&\quad - iak\zeta_k - \gamma k^2 \zeta_k
\end{aligned} \tag{2.19}$$

and

$$\begin{aligned}
\dot{\zeta}_k - |k|\phi_k &= \sum_{\ell, p} \ell p \phi_\ell \zeta_p \int e^{|\ell|\zeta(x)} \chi_\ell \chi_p \chi_k^* dx \\
&\quad + \sum_{\ell} |\ell| \phi_\ell \int (e^{|\ell|\zeta(x)} - 1) \chi_\ell \chi_k^* dx
\end{aligned} \tag{2.20}$$

or defining $F_1(k)$ and $F_2(k)$ by the right hand sides of Eqs. (2.19) and (2.20), respectively, we have the set of equations

$$\dot{\phi}_k + G_k \zeta_k = F_1(k) \tag{2.21}$$

where $G_k \equiv g + \gamma k^2$ and

$$\dot{\zeta}_k - |k|\phi_k = F_2(k) \tag{2.22}$$

which to this point provides a formally exact description of the interaction process in a single horizontal dimension.

We now return to the discussion of the viscous damping of high frequency waves. In a viscous fluid the interaction between water molecules produces shearing effects when the water is in motion and destroys the irrotational assumption imposed above. In such a system we assume that we can superimpose the rotational character of the fluid on the irrotational so that

$$\vec{u} = \nabla\phi + \vec{u}' \quad (2.23)$$

where $\nabla \times \vec{u}' \neq 0$.

The energy of the fluid motion is gradually dissipated by these shearing effects and may be modeled by determining the rate at which the energy is being dissipated.

Following Phillips' discussion of viscosity, we write the rate of strain tensor as

$$e_{ij} = \frac{1}{2} \left\{ \frac{\partial u_i}{\partial x_j} + \frac{\partial u_j}{\partial x_i} \right\} \quad (2.24)$$

where $(i,j = 1,2)$ label the components of the coordinate system and velocity. Assuming the ocean to be an isotropic, incompressible Newtonian fluid, and μ to be the coefficient of viscosity, we may write the frictional force per unit volume in terms of the derivative of the rate of strain tensor, i.e.

$$f_i = \mu \frac{\partial e_{ij}}{\partial x_j} \quad (2.25)$$

since $\nabla \cdot \vec{u} = 0$. We may also write the rate of working against viscous forces as

$$\begin{aligned} u_i f_i &= 2\mu u_i \frac{\partial e_{ij}}{\partial x_j} \\ &= 2\mu \frac{\partial}{\partial x_j} (u_i e_{ij}) - \epsilon \end{aligned} \quad (2.26)$$

$$\text{where } \epsilon = 2\mu (e_{ij})^2 = 2\mu e_{ij} \frac{\partial u_i}{\partial x_j} \quad (2.27)$$

The first term on the right of Eq. (2.26) represents the viscous energy flux; the second term, the rate of energy dissipation per unit volume by molecular viscosity.

The rate of energy dissipation per unit area at the surface of a very deep ocean can be written, using Eq. (2.26)

$$\dot{E} = - \int_{-\infty}^{\zeta} \epsilon dz = - \int_{-\infty}^{\zeta} \frac{1}{2}\mu \left\{ \frac{\partial u_i}{\partial x_j} + \frac{\partial u_j}{\partial x_i} \right\}^2 dz \quad (2.28)$$

The contribution from the surface layer is assumed to be small, the primary effect coming from the ocean interior.

Using only the irrotational part of the velocity from Eq. (2.23), we may write Eq. (2.28) up to second order as

$$\dot{E} = - \int_{-\infty}^0 2\mu \left[\frac{\partial^2 \phi}{\partial x_i \partial x_j} \right]^2 dz \quad (2.29)$$

We evaluate Equation (2.29) using a single mode solution to the linear equation, i.e.,

$$\phi = c \phi_k e^{kz} \sin [k(x - ct)] \quad (2.30)$$

so that Equation (2.29) is reduced to

$$\dot{E} = - 2\mu \phi_k^2 k^3 c^2 \quad (2.31)$$

Using the fact that in deep water

$$E = \frac{1}{2} \rho \phi_k^2 c^2 k$$

the attenuation coefficient γ_v for this wave can be written as

$$\gamma_v = - \frac{\dot{E}}{2E} = 2\nu k^2 \quad (2.32)$$

where $\nu = \mu/\rho$ is the kinematic viscosity of water. The energy density of the wave field decreases as $\exp \{-2\gamma_v t\}$ and the amplitude by $\exp \{-\gamma_v t\}$. We may, therefore, model the effect of viscosity in Equation (2.21) by including the term

$$-2\nu k^2 \phi_k \quad (2.33)$$

in $F_1(k)$.

The equations for the ocean surface now take the form

$$\dot{\phi}_k + G_k \zeta_k = F_1(k) - 2\nu k^2 \phi_k = \hat{F}_1(k) \quad (2.34)$$

and

$$\dot{\zeta}_k - |k| \phi_k = F_2(k) = \hat{F}_2(k) \quad (2.35)$$

which includes models for: (i) the generation of waves by wind, (ii) the non-linear interaction of surface waves, (iii) the effect of damping by the dissipation of energy through molecular viscosity, and (iv) the generation of capillary waves.

3. EIGENMODE DESCRIPTION

The structure of Eqs. (2.34) and (2.35) suggests that it may be possible to transform these coupled equations to a decoupled representation. We can in fact define the new variables

$$\phi_k = \sqrt{G_k} \psi_1(k) \quad (3.1a)$$

and

$$\zeta_k = i \sqrt{|k|} \psi_2(k) \quad (3.1b)$$

which, when substituted into Equations (2.34) and (2.35), yield

$$i\dot{\psi}_1(k) - \sqrt{G_k|k|} \psi_2(k) = \frac{i}{\sqrt{G_k}} \hat{F}_1(k) \quad (3.2a)$$

and

$$i\dot{\psi}_2(k) - \sqrt{G_k|k|} \psi_1(k) = \frac{1}{\sqrt{|k|}} \hat{F}_2(k) \quad (3.2b)$$

If we take the sum and difference of Eqs. (3.2a) and (3.2b), we obtain

$$i(\dot{\psi}_1 + \dot{\psi}_2) - \sqrt{G_k|k|} (\psi_1 + \psi_2) = \frac{i}{\sqrt{G_k}} \hat{F}_1(k) + \frac{1}{\sqrt{|k|}} \hat{F}_2(k)$$

and

$$i(\dot{\psi}_1 - \dot{\psi}_2) + \sqrt{G_k|k|} (\psi_1 - \psi_2) = \frac{i}{\sqrt{G_k}} \hat{F}_1(k) - \frac{1}{\sqrt{|k|}} \hat{F}_2(k)$$

which in terms of the quantities

$$b_k^{(\pm)} \equiv \frac{1}{\sqrt{2}} [\psi_1(k) \pm \psi_2(k)] \left(\frac{|k|^3}{L} \right)^{\frac{1}{2}} = \frac{1}{\sqrt{2G_k}} \left[\phi_k \mp i \sqrt{\frac{G_k}{|k|}} \zeta_k \right] \left(\frac{|k|^3}{L} \right)^{\frac{1}{2}} \quad (3.3)$$

and

$$F^{(\pm)}(k) = \left[\frac{i}{\sqrt{2G_k}} \hat{F}_1(k) \pm \frac{1}{\sqrt{2|k|}} \hat{F}_2(k) \right] \left(\frac{|k|^3}{L} \right)^{\frac{1}{2}} \quad (3.4)$$

becomes

$$i\dot{b}_k^{(+)} - \sqrt{G_k|k|} b_k^{(+)} = F^{(+)}(k) \quad (3.5a)$$

and

$$i\dot{b}_k^{(-)} + \sqrt{G_k|k|} b_k^{(-)} = F^{(-)}(k) \quad (3.5b)$$

In terms of the orthonormal matrices

$$\underline{\zeta}^{(+)} = \frac{1}{\sqrt{2}} \begin{pmatrix} 1 \\ 1 \end{pmatrix} \quad \text{and} \quad \underline{\zeta}^{(-)} = \frac{1}{\sqrt{2}} \begin{pmatrix} 1 \\ -1 \end{pmatrix}$$

Eqs. (3.3) to (3.5) can be written

$$b_k = b_k^{(+)} \underline{\zeta}^{(+)} + b_k^{(-)} \underline{\zeta}^{(-)} \quad (3.6)$$

$$\underline{F}(k) = F(k) \underline{\zeta}^{(+)} + F(k) \underline{\zeta}^{(-)} \quad (3.7)$$

and

$$i\dot{\underline{b}}_k - \underline{\Delta} \underline{b}_k = \underline{F}(k) \quad (3.8)$$

where

$$\underline{\Delta} \underline{\zeta}^{(\pm)} = \pm \sqrt{G_k|k|} \underline{\zeta}^{(\pm)} \quad (3.9)$$

Using the preceeding equations, we may express the velocity potential and wave height in terms of the eigenmode amplitudes of the problem $[b_k^{(\pm)}]$ as follows

$$\phi_k = \sqrt{G_k} \psi_1(k) = \sqrt{\frac{G_k}{2}} \{b_k^{(+)} + b_k^{(-)}\} \left(\frac{L}{|k|^3}\right)^{\frac{1}{2}} \quad (3.10)$$

and

$$\zeta_k = i \sqrt{|k|} \quad \psi_2(k) = i \sqrt{\frac{|k|}{2}} \{b_k^{(+)} - b_k^{(-)}\} \left(\frac{L}{|k|^3}\right)^{\frac{1}{2}}. \quad (3.11)$$

Both the velocity potential and the wave height are real quantities so we may equate them with their respective complex conjugates

$$\begin{aligned} \phi &= \phi^* = \sum_k \chi_k e^{ikz} \sqrt{\frac{G_k}{2}} \{b_k^{(+)} + b_k^{(-)}\} \left(\frac{L}{|k|^3}\right)^{\frac{1}{2}} \\ &= \sum_k \chi_k^* e^{ikz} \sqrt{\frac{G_k}{2}} \{b_k^{(+)*} + b_k^{(-)*}\} \left(\frac{L}{|k|^3}\right)^{\frac{1}{2}} \end{aligned}$$

and because $\chi_k^* = \chi_{-k}$ we obtain

$$b_k^{(+)} + b_k^{(-)} = b_{-k}^{(+)*} + b_{-k}^{(-)*} \quad (3.12a)$$

In a similar manner

$$\begin{aligned} \zeta^* &= \zeta = + i \sum_k \sqrt{\frac{|k|}{2}} \chi_k \{b_k^{(+)} - b_k^{(-)}\} \left(\frac{L}{|k|^3}\right)^{\frac{1}{2}} \\ &= - i \sum_k \sqrt{\frac{|k|}{2}} \chi_k^* \{b_k^{(+)*} - b_k^{(-)*}\} \left(\frac{L}{|k|^3}\right)^{\frac{1}{2}}. \end{aligned}$$

and therefore

$$i(b_k^{(+)} - b_k^{(-)}) = -i(b_{-k}^{(+)*} - b_{-k}^{(-)*}) \quad (3.12b)$$

Adding and subtracting Equation (3.12) yields the following conditions on the amplitudes

$$b_k^{(+)} = b_{-k}^{(-)*} \quad ; \quad b_k^{(-)} = b_{-k}^{(+)*} \quad . \quad (3.13)$$

We can remove the rapidly oscillating part of the expression in our eigenmode equations [Equation (3.5)] by introducing the variables

$$b_k^{(\pm)} = \frac{q_k^{(\pm)}}{\sqrt{2}} e^{\mp i\omega_k t} \quad (3.14)$$

where $q_k^{(\pm)}$ is assumed to be a slowly varying function of time. If we equate ω_k to $\sqrt{G_k|k|}$ in Eq. (3.5), then we have the new equations

$$i\dot{q}_k^{(\pm)} = e^{\pm i\omega_k t} F^{(\pm)}(k) \sqrt{2} \quad (3.15)$$

for our system.

To interpret the significance of the $q_k^{(\pm)}$, let us consider a single mode propagating to the right. Then, according to Eq. (2.14) the wave height is

$$\zeta(x,t) = \chi_k(x) \zeta_k(t) + \chi_{-k}(x) \zeta_{-k}(t) \quad .$$

Taking $b_k^{(+)}$ and $b_{-k}^{(-)} = [b_k^{(+)}]^*$ as the only nonvanishing modes, this becomes

$$\zeta(x, t) = \left(\frac{i}{2|k|} \right) \left[q_k^{(+)} e^{i(kx - \omega_k t)} - q_k^{(+)*} e^{-i(kx - \omega_k t)} \right].$$

On setting $\lambda \equiv |k|^{-1}$ and

$$q_k^{(+)} = |q_k^{(+)}| e^{i\theta_k},$$

this becomes

$$\frac{\zeta(x, t)}{\lambda} = -|q_k^{(+)}| \sin[kx - \omega_k t + \theta_k]. \quad (3.16)$$

The dimensionless quantity $|q_k^{(+)}|$ thus represents the ratio of the maximum wave amplitude to λ . We expect $0 < |q_k^{(\pm)}| < 1$, since at the upper limit very strong coupling between modes will occur. This notion is consistent with the analysis done by Stokes on finite amplitude effects on gravity waves in deep water. It was determined that a maximum crest angle (120°) for gravity waves existed, after which the wave becomes unstable. This restriction is easily maintained in terms of the slope of the gravity wave, i.e., the ratio given by Equation (3.16). The quantity $q_k^{(+)}$ is, therefore, a more natural variable for the problem than the wave height.

3A. The Approximate Equations

Although Eq. (3.15) is formally exact, in its present form it is not of much use. It may be put in a more manageable form for numerical calculation by making a number of reasonable approximations. Consider the function $\hat{F}_1(k)$,

$$\begin{aligned} \hat{F}_1(k) = & \frac{1}{2} \sum_{\ell, p} (\ell p - |\ell| |p|) \phi_\ell \phi_p \int e^{(|\ell| + |p|) \zeta(x)} \chi_\ell \chi_p^* dx \\ & - \sum_{\ell} \dot{\phi}_\ell \int (e^{|\ell| \zeta(x)} - 1) \chi_\ell \chi_k^* dx - i \alpha k \zeta_k - 2 \nu k^2 \phi_k \end{aligned} \quad (3.17)$$

in this expression the function ζ multiplied by a wavenumber in the exponential is a small quantity since the slope cannot exceed the value $1/7$. This value is a result of the Stokes analysis mentioned earlier. The wavenumber in the exponential is generally restricted to a region of wavenumber space in which the surface elevation is being expanded, i.e., $|k_{\min}| \leq |\ell| \leq |k_{\max}|$ and $|k_{\min} - k_{\max}| \ll |\ell|$, so that $|\ell| \zeta(x)$ has a critical value which is on the order of $2\pi/7 \approx 1$. It is therefore not unreasonable to expand the exponentials under the integral sign in Equation (3.17) and keep terms to only third order in the amplitudes when one is not considering capillary waves or those gravity waves close to breaking.

We perform this expansion in Equation (3.17) and replace ζ by its Fourier expansion [Equation (2.14)] to obtain,

$$\begin{aligned}
\hat{F}_1(k) \approx & \frac{1}{2} \sum_{\ell+p=k} \frac{(\ell p - |\ell||p|)\phi_\ell\phi_p}{\sqrt{L}} - \sum_{\ell+p=k} \frac{|\ell|\dot{\phi}_\ell\zeta_p - iak\zeta_k}{\sqrt{L}} \\
& + \sum_{\ell+p+n=k} \frac{\frac{1}{2}(\ell p - |\ell||p|)(|\ell| + |p|)\phi_\ell\phi_p\zeta_n - 2vk^2\phi_k}{\sqrt{L}} \\
& - \sum_{\ell+p+n=k} \frac{\frac{|\ell|^2}{2}\dot{\phi}_\ell\zeta_p\zeta_n}{\sqrt{L}}. \quad (3.18)
\end{aligned}$$

The time derivatives of the amplitudes may be replaced in this expression by their value from Eq. (2.19) to obtain

$$\begin{aligned}
\hat{F}_1(k) \approx & -iak\zeta_k - 2vk^2\phi_k \\
& + \sum_{\ell+p=k} \frac{\left\{ \frac{1}{2}(\ell p - |\ell||p|)\phi_\ell\phi_p + (G_\ell + i\alpha\ell)|\ell|\zeta_\ell\zeta_p \right.}{\sqrt{L}} \\
& \quad \left. + 2v\ell^2\phi_\ell\zeta_p \right\} \\
& + \sum_{\ell+p+n=k} \frac{\left\{ \frac{1}{2}(\ell p - |\ell||p|)(|\ell| + |p| - |\ell+p|)\phi_\ell\phi_p\zeta_n \right.}{\sqrt{L}} \\
& \quad \left. + \frac{|\ell|^2}{2}[(G_\ell + i\alpha\ell)\zeta_\ell + 2v\ell^2\phi_\ell]\zeta_p\zeta_n \right\}. \quad (3.19)
\end{aligned}$$

In a similar way we obtain the following expression for $\hat{F}_2(k)$

$$\hat{F}_2(k) \approx \sum_{\ell+p=k} \frac{\ell(\ell+p)\phi_\ell\zeta_p}{\sqrt{L}} + \sum_{\ell+p+n=k} \frac{\left\{ \ell p + \frac{|\ell|^2}{2} \right\} |\ell|\phi_\ell\zeta_p\zeta_n}{\sqrt{L}}. \quad (3.20)$$

Our eigenmode equations are, however, in terms of $q_k^{(\pm)}$ and $F^{(\pm)}(k)$ not ϕ_k , ζ_k and $\hat{F}(k)$. We must therefore determine $F^{(\pm)}$ in terms of $q_k^{(\pm)}$.

We recall that

$$F^{(\pm)}(k) = \left\{ \frac{i}{\sqrt{2G_k}} \hat{F}_1(k) \pm \frac{1}{\sqrt{2|k|}} \hat{F}_2(k) \right\} \left(\frac{|k|^3}{L} \right)^{\frac{1}{2}}$$

which may be written using Eqs. (3.19) and (3.20) and Eqs. (3.10) and (3.11);

$$\begin{aligned} \sqrt{2G_k} F^{(\pm)}(k) = & \sum_{l+p=k} \left\{ \alpha_{lp} [b_l^{(+)} + b_l^{(-)}] [b_p^{(+)} + b_p^{(-)}] \right. \\ & + \beta_{lp} [b_l^{(+)} - b_l^{(-)}] [b_p^{(+)} - b_p^{(-)}] \\ & + \gamma_{lp;k}^{(\pm)} [b_l^{(+)} + b_l^{(-)}] [b_p^{(+)} - b_p^{(-)}] \left. \right\} \left(\frac{|k|}{Lp} \right)^{\frac{3}{2}} \\ & + \sum_{l+p+n=k} \left\{ \alpha_{lpn} [b_l^{(+)} + b_l^{(-)}] [b_p^{(+)} + b_p^{(-)}] [b_n^{(+)} - b_n^{(-)}] \right. \\ & + \beta_{lpn} [b_l^{(+)} - b_l^{(-)}] [b_p^{(+)} - b_p^{(-)}] [b_n^{(+)} - b_n^{(-)}] \\ & + \gamma_{lpn;k}^{(\pm)} [b_l^{(+)} + b_l^{(-)}] [b_p^{(+)} - b_p^{(-)}] [b_n^{(+)} - b_n^{(-)}] \left. \right\} \left(\frac{|k|}{Lpn} \right)^{\frac{3}{2}} \\ & + i\alpha k \sqrt{\frac{|k|}{2}} [b_k^{(+)} - b_k^{(-)}] - 2ivk^2 \sqrt{\frac{G_k}{2}} [b_k^{(+)} + b_k^{(-)}] \end{aligned} \quad (3.20)$$

and

$$\begin{aligned} \alpha_{lp} &= \left\{ \frac{i\sqrt{G_l G_p}}{4} (lp - |l||p|) \right\}, \\ \beta_{lp} &= -i \frac{|l|}{2} \sqrt{|l||p|} (G_l + i\alpha l), \\ \gamma_{lp;k}^{(\pm)} &= -v l^2 \sqrt{G_l |p|} \pm i \frac{\sqrt{G_k G_l}}{2} \sqrt{\frac{|p|}{|k|}} l(l+p), \end{aligned}$$

$$\alpha_{lpn} = - \frac{\sqrt{G_l G_p}}{4} (lp - |l| |p|) (|l| + |p| - |l+p|) \sqrt{|n|/2} ,$$

$$\beta_{lpn} = \frac{|l|^2}{4} \sqrt{|l| |p| |n|/2} (G_l + i\alpha l) ,$$

and

$$\gamma_{lpn;k}^{(\pm)} = \sqrt{\frac{G_l}{2}} \left\{ -i v l^4 + \left(lp + \frac{l^2}{2} \right) |l| \sqrt{\frac{G_k}{|k|}} \right\} \frac{\sqrt{|p| |n|}}{2} . \quad (3.22)$$

The complete expression for Equation (3.16) is as follows:

$$\begin{aligned} \sqrt{G_k} i \dot{q}_k^{(\pm)} e^{\mp i \omega_k t} = & \sum_{l+p=k} \frac{1}{2} \left\{ q_l^{(+)} q_p^{(+)} e^{-i(\omega_l + \omega_p)t} \left[\alpha_{lp} + \beta_{lp} + \gamma_{lp;k}^{(\pm)} \right] \right. \\ & + q_l^{(-)} q_p^{(-)} e^{i(\omega_l + \omega_p)t} \left[\alpha_{lp} + \beta_{lp} - \gamma_{lp;k}^{(\pm)} \right] \\ & + q_l^{(+)} q_p^{(-)} e^{-i(\omega_l - \omega_p)t} \left[\alpha_{lp} - \beta_{lp} - \gamma_{lp;k}^{(\pm)} \right] \\ & + q_l^{(-)} q_p^{(+)} e^{i(\omega_l - \omega_p)t} \left[\alpha_{lp} - \beta_{lp} + \gamma_{lp;k}^{(\pm)} \right] \left. \right\} \left(\left| \frac{k}{pl} \right| \right)^{3/2} \\ & + \frac{1}{\sqrt{8}} \sum_{l+p+n=k} \left\{ q_l^{(+)} q_p^{(+)} q_n^{(+)} e^{-i(\omega_l + \omega_p + \omega_n)t} \left[\alpha_{lpn} + \beta_{lpn} + \gamma_{lpn;k}^{(\pm)} \right] \right. \\ & + q_l^{(+)} q_p^{(+)} q_n^{(-)} e^{-i(\omega_l + \omega_p - \omega_n)t} \left[-\alpha_{lpn} - \beta_{lpn} - \gamma_{lpn;k}^{(\pm)} \right] \\ & + q_l^{(+)} q_p^{(-)} q_n^{(+)} e^{-i(\omega_l - \omega_p + \omega_n)t} \left[\alpha_{lpn} - \beta_{lpn} - \gamma_{lpn;k}^{(\pm)} \right] \\ & + q_l^{(-)} q_p^{(-)} q_n^{(-)} e^{i(\omega_l - \omega_p - \omega_n)t} \left[-\alpha_{lpn} + \beta_{lpn} + \gamma_{lpn;k}^{(\pm)} \right] \left. \right\} \left(\left| \frac{k}{pnl} \right| \right)^{3/2} \end{aligned}$$

$$\begin{aligned}
& + q_l^{(+)} q_p^{(-)} q_n^{(-)} e^{-i(\omega_l - \omega_p - \omega_n)t} \left[-\alpha_{lpn} + \beta_{lpn} + \gamma_{lpn;k}^{(\pm)} \right] \\
& + q_l^{(-)} q_p^{(+)} q_n^{(+)} e^{i(\omega_l - \omega_p - \omega_n)t} \left[\alpha_{lpn} - \beta_{lpn} + \gamma_{lpn;k}^{(\pm)} \right] \\
& + q_l^{(-)} q_p^{(+)} q_n^{(-)} e^{i(\omega_l - \omega_p + \omega_n)t} \left[-\alpha_{lpn} + \beta_{lpn} - \gamma_{lpn;k}^{(\pm)} \right] \\
& + q_l^{(-)} q_p^{(-)} q_n^{(+)} e^{i(\omega_l + \omega_p - \omega_n)t} \left[\alpha_{lpn} + \beta_{lpn} - \gamma_{lpn;k}^{(\pm)} \right] \\
& + q_l^{(-)} q_p^{(-)} q_n^{(-)} e^{i(\omega_l + \omega_p + \omega_n)t} \left[-\alpha_{lpn} - \beta_{lpn} + \gamma_{lpn;k}^{(\pm)} \right] \Big\} \\
& \pm \left\{ iak \sqrt{\frac{|k|}{2}} \mp 2ivk \sqrt{\frac{G_k}{2}} \right\} \frac{q_k^{(\pm)}}{\sqrt{2}} e^{\mp i\omega_k t} \quad (3.23)
\end{aligned}$$

3B. The Resonance Condition

We expect that in the development of the amplitude of the k^{th} mode non-resonant terms, being oscillatory, will make a zero, i.e., negligible, net contribution for the interaction of surface gravity waves alone. Only those combination of frequency close to ω_k , i.e., those in resonance, will contribute substantially to $q_k^{(\pm)}$. We therefore rewrite Equation (3.23) for a right travelling wave as

$$\begin{aligned}
\dot{q}_k^{(+)} &= \left[\frac{\alpha k |k|}{2\omega_k} - vk^2 \right] q_k^{(+)} \\
&+ \frac{i}{2} \sum_{l+p=k+n} \left\{ \left[\alpha_{lp-n} + \beta_{lp-n} + \gamma_{lp-n;k}^{(+)} \right] q_l^{(+)} q_p^{(+)} q_{-n}^{(-)} \right. \\
&- \left[\alpha_{l-np} - \beta_{l-np} - \gamma_{l-np;k}^{(+)} \right] q_l^{(+)} q_{-n}^{(-)} q_p^{(+)} \\
&- \left. \left[\alpha_{-npl} - \beta_{-npl} + \gamma_{-npl;k}^{(+)} \right] q_{-n}^{(-)} q_p^{(+)} q_n^{(+)} \right\} \times \\
&\times \left[\frac{1}{2G_k} \left| \frac{k}{lpn} \right|^3 \right]^{\frac{1}{2}} \exp \left\{ i(\omega_k + \omega_n - \omega_l - \omega_p)t \right\}
\end{aligned}$$

which we can rewrite in the form

$$\begin{aligned}
\dot{q}_k^{(+)} &= \left[\frac{\alpha k |k|}{2\omega_k} - vk^2 \right] q_k^{(+)} \\
&+ \sum_{l+p=k+n} i \Gamma_{lpn;k} q_l^{(+)} q_p^{(+)} q_{-n}^{(-)} e^{i\Omega_{lpnk}t}
\end{aligned} \tag{3.24}$$

where

$$\begin{aligned}
\Gamma_{lpn;k} &= \frac{1}{2} \left(\alpha_{lp-n} + \beta_{lp-n} - \gamma_{lp-n;k}^{(+)} - \alpha_{l-np} + \beta_{l-np} + \gamma_{l-np;k}^{(+)} \right. \\
&- \left. \alpha_{-npl} + \beta_{-npl} - \gamma_{-npl;k}^{(+)} \right) \left(\frac{1}{2G_k} \left| \frac{k}{lpn} \right|^3 \right)^{\frac{1}{2}}
\end{aligned} \tag{3.25}$$

and

$$\Omega_{\ell p n k} = \omega_k + \omega_n - \omega_\ell - \omega_p \quad (3.26)$$

If we define the functions

$$H_{\ell p n}(t) = q_\ell^{(+)} q_p^{(+)} [q_n^{(+)}]^* \quad (3.27)$$

and

$$\Omega = \Omega_{\ell p n k} \quad (3.28)$$

then Equation (3.24) can be written in the form

$$\dot{q}_k^{(+)} = \left[\frac{\alpha k |k|}{2\omega_k} - \nu k^2 \right] q_k^{(+)} + \sum_{\ell+p=k+n} i \Gamma_{\ell p n; k} H_{\ell p n}(t) e^{i\Omega t} \quad (3.29)$$

where

$$\Gamma_{\ell p n; k} = R_{\ell p n; k} + i I_{\ell p n; k}$$

$$\begin{aligned} R_{\ell p n; k} = & \frac{\omega_k}{16G_k} \frac{|k|}{|\ell p n|^{3/2}} \times \\ & \times \left\{ \sqrt{G_\ell G_p} (|\ell p| - \ell p) (|\ell| + |p| - |\ell+p|) \sqrt{|n|} \right. \\ & - \sqrt{G_\ell G_n} (|\ell n| + \ell p) (|\ell| + |n| - |\ell-n|) \sqrt{|p|} \\ & - \sqrt{G_n G_p} (|np| + np) (|n| + |p| - |n-p|) \sqrt{|\ell|} \\ & + (|\ell p n|)^{\frac{1}{2}} \left(G_n n^2 + 2G_\ell \ell^2 \right) + (n^2 - 2np) |n| \left(\left| \frac{p\ell}{k} \right| \right)^{\frac{1}{2}} \sqrt{G_n G_k} \\ & \left. - \sqrt{G_\ell G_k} \ 2\ell (\ell - n + p) |\ell| \left(\left| \frac{pn}{k} \right| \right)^{\frac{1}{2}} \right\} \end{aligned}$$

$$I_{\ell pn; k} = \frac{\omega_k}{16G_k} \frac{|k|}{|\ell pn|^{3/2}} \left[\alpha |\ell pn|^{\frac{1}{2}} 2\ell^3 - n^3 + 2v \left(\sqrt{G_n} n^4 |p\ell|^{\frac{1}{2}} - 2\sqrt{G_\ell} \ell^4 |pn|^{\frac{1}{2}} \right) \right]. \quad (3.30)$$

The numerical integration of Equation (3.29) is discussed in Appendix A.

4. DISCUSSION OF EQUATION (3.29)*

The wavenumbers in the interval $0 < x < L$ are of the form

$$k = \frac{2\pi}{L} K, \quad p = \frac{2\pi}{L} P, \quad \text{etc.}, \quad (4.1)$$

where K, P , etc., are integers. The wavenumber matching condition in Equation (3.24) using Equation (4.1) is then an integer matching condition.

The quantity Γ [Equation (3.30)] has the dimensions of a frequency and is of the same order of magnitude as the mode frequency, that is,

$$\Gamma = O(\omega_k) \quad , \quad (4.2)$$

where ω_k is a characteristic wave angular frequency in the wavenumber region of interest. We recall that the $q_k^{(\pm)}$ are dimensionless ratios of [from Equation (3.16)],

$$\frac{\text{wave height}}{\text{wave length}} \frac{2\pi}{\text{wave length}} \quad .$$

When the q_k 's are nearly unity, the non-linear interaction has a time constant comparable to the wave period.

When the q_k 's are small compared with unity, the characteristic time constant of the non-linear terms is $\sim [\omega_k |a|^2]^{-1}$.

* In this Section we set $G_k \approx g$, i.e., neglect surface tension.

When

$$|\Omega_{\ell p n k}| \gg [\omega_k |a|^2] \quad (4.3)$$

the oscillating exponential will tend to "wash out" the non-linear coupling.

If we set [assume $\ell, p, k, n \geq 0$]

$$k = \ell - \eta$$

$$n = p + \eta, \quad (4.4)$$

we satisfy the wavenumber matching condition $k + n = \ell + p$. The frequency mismatch (3.26) is then

$$\Omega = -\sqrt{g} \left[\sqrt{\ell} + \sqrt{p} - \sqrt{\ell - \eta} - \sqrt{p + \eta} \right], \quad (4.5)$$

$$-p < \eta < \ell. \quad (4.6)$$

Next, we assume $\ell \geq p$ and write

$$q \equiv \frac{p}{\ell}, \quad y \equiv \frac{\eta}{\ell}, \quad -q < y < 1, \quad (4.7)$$

to obtain

$$-\frac{\Omega}{\omega_\ell} \equiv f(q, y) = 1 + \sqrt{q} - \sqrt{1-y} - \sqrt{q+y}. \quad (4.8)$$

At the y -end points f is positive and has the value

$$f(q, -q) = f(q, 1) = \frac{2\sqrt{q}}{1 + \sqrt{q} + \sqrt{1+q}} \quad (4.9)$$

f has two, and only two, zeros. These occur at

$$\eta = 0, \quad \eta = l - p. \quad (4.10)$$

Between these zeros f is negative and has the minimum value

$$f_{\min}(q) = f\left(q, \frac{1-q}{2}\right) = - \frac{(1 - \sqrt{q})^2}{1 + \sqrt{q} + \sqrt{2(1-q)}}$$

The quantity $f_{\min}(q)$ is plotted in Figure 1.

For the self-interaction of a single mode, we have

$$\Gamma_k \equiv \Gamma_{kkk;k} = -\frac{\omega_k}{2} \left[1 - i \left(\frac{\alpha k}{8g} - \frac{\nu k^2}{4\omega_k} \right) \right]. \quad (4.12)$$

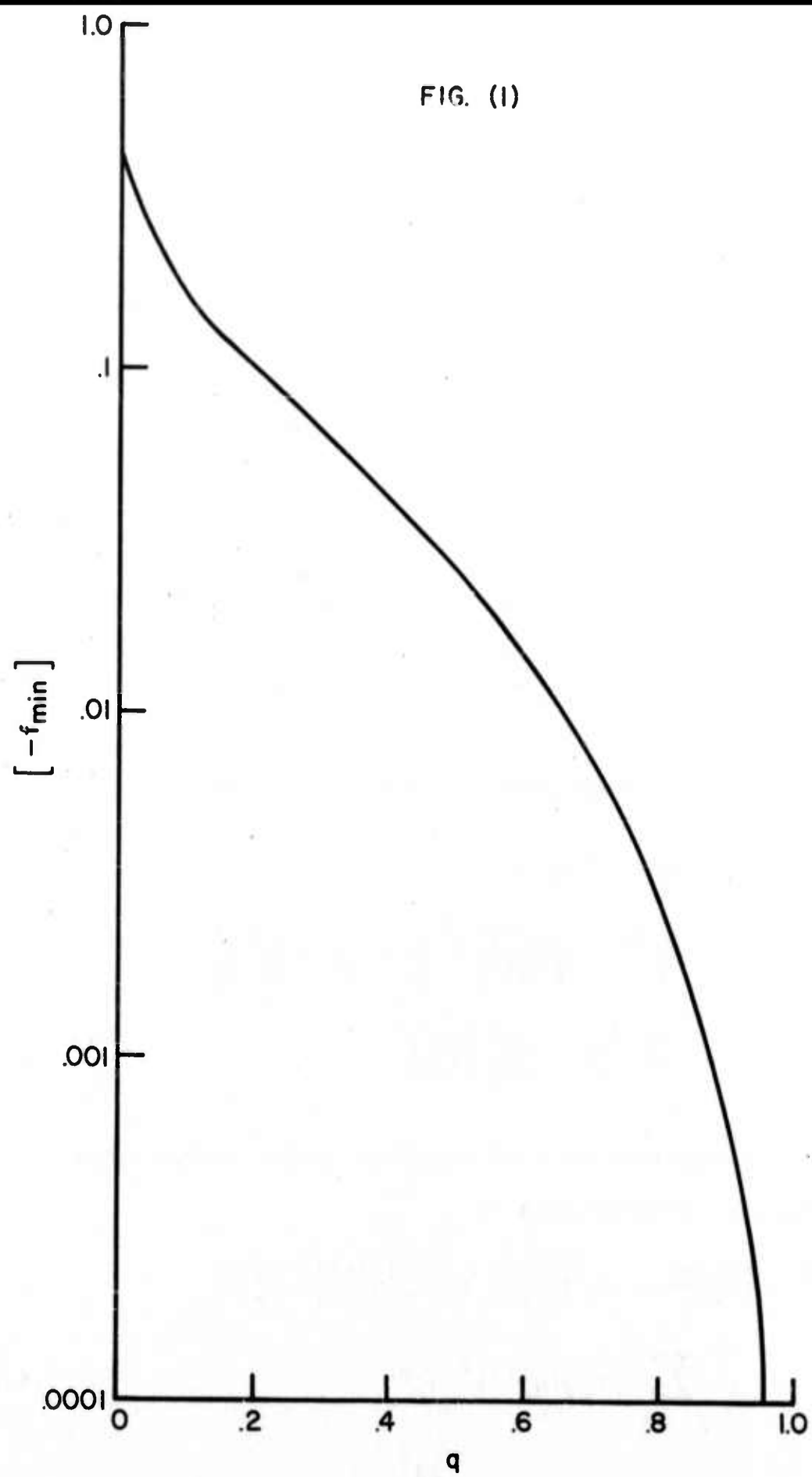
For scattering with no change of wavenumber, we have

$$\begin{aligned} \Gamma_{nk} &\equiv \Gamma_{nkn;k} + \Gamma_{knn;k} \\ &= -\frac{\omega_k}{4} \left[1 + \sqrt{\left| \frac{k}{n} \right|} \left(2 + \frac{k}{n} - \left| 1 - \frac{k}{n} \right| \right) \right] \\ &\quad + \frac{i\omega_k}{2} \left(\frac{\alpha k}{4g} - \frac{\nu k^2}{2\omega_k} \right) \left(\frac{k}{n} \right)^2 \end{aligned} \quad (4.13)$$

The appropriate form of Equation (3.24) in the case of pure resonant interactions is

$$\begin{aligned} \dot{q}_k^{(+)} &= \left(\frac{\alpha k |k|}{2\omega_k} - \nu k^2 \right) q_k^{(+)} + i\Gamma_k |q_k^{(+)}|^2 q_k^{(+)} \\ &\quad + \sum_{n(\neq k)} i\Gamma_{nk} |q_n^{(+)}|^2 q_k^{(+)} \end{aligned} \quad (4.14)$$

FIG. (I)



The quantity $[-\Gamma_{nk}/\omega_k]$ is plotted in Fig. (2) as a function of the ratio (k/n) for the case $\alpha = \nu = 0$.

Let us consider the rate equation for the self-interaction of a single mode in the absence of wind and neglecting viscosity, i.e.,

$$\dot{q}_k^{(+)} = -i \frac{\omega_k}{2} |q_k^{(+)}|^2 q_k^{(+)} \quad (4.15)$$

where we have used Equations (4.12) and (4.14). We may pre-multiply Equation (4.15) by $q_k^{(+)*}$ and premultiply the complex conjugate of Equation (4.15) by $q_k^{(+)}$ and add the two equations to obtain

$$\frac{d}{dt} |q_k^{(+)}|^2 = 0 \quad (4.16)$$

which implies that the modulus of $q_k^{(+)}$ is constant. We therefore write

$$q_k^{(+)} = c_k e^{i\chi_k} \quad (4.17)$$

where c_k is constant. Substituting Equation (4.17) into Equation (4.15) we obtain

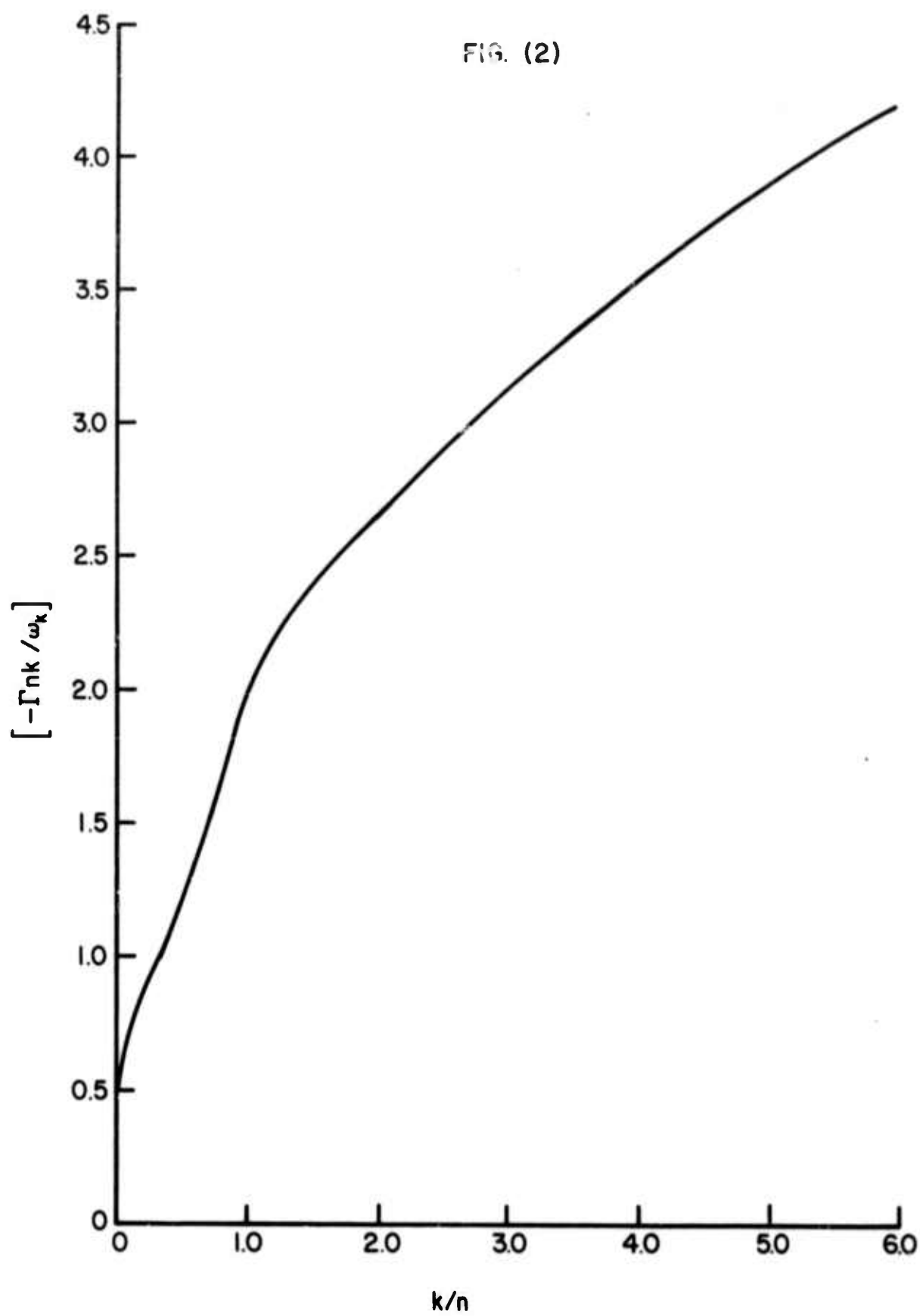
$$\dot{\chi}_k = -\frac{\omega_k}{2} |c_k|^2 \quad (4.18)$$

which yields

$$q_k^{(+)} = c_k \exp \left\{ -i \frac{\omega_k}{2} |c_k|^2 t \right\} \quad (4.19)$$

as the solution to the interaction equation for a single mode [Equation (4.15)].*

* Note that this result will not change if the Γ_{nk} terms in Equation (4.14) are also included in Equation (4.15).



In this single mode case we can write the velocity potential in terms of its Fourier amplitudes [Equation (4.19)] as

$$\phi_k = \left(\frac{G_k L}{2|k|^3} \right)^{\frac{1}{2}} \left\{ c_k e^{-i\omega_k \left[1 + \frac{1}{2}|c_k|^2 \right] t} + c_k^* e^{i\omega_k \left[1 + \frac{1}{2}|c_k|^2 \right] t} \right\}. \quad (4.20)$$

We can use Equation (4.20) to write the phase velocity for this single wave as

$$c_{ph} = \frac{\omega_k + \Delta\omega_k}{k} = \sqrt{g/k} \left\{ 1 + \frac{1}{2}|c_k|^2 \right\} \quad (4.21)$$

in terms of the modulus of the mode amplitude. From Equation (4.17) it is clear that $c_k = q_k^{(+)}(t=0)$, so that,

$$|c_k|^2 = |q_k^{(+)}(t=0)|^2 = k^2 \zeta^2 \quad (4.22)$$

where we have used Equation (3.16) to write the second equality in Equation (4.22). The phase velocity may therefore be written as

$$c_{ph} = \sqrt{g/k} \left\{ 1 + \frac{1}{2} k^2 \zeta^2 \right\} \quad (4.23)$$

which is seen to agree to second order with the phase velocity of a Stokes wave, i.e., have the appropriate amplitude dependence.

5. SEA SURFACE CONTOUR AND ENERGY

Consistent with the spirit of our technique, which assumes the non-linear couplings to be relatively weak, we shall calculate the wave energy to only second order in the wave amplitude. The kinetic and potential energies per unit surface area are, respectively,

$$\text{K.E.} = \frac{1}{L} \int_0^L dx \int_{-\infty}^{\zeta} \frac{1}{2} \rho u^2 dz, \quad (5.1)$$

and

$$\text{P.E.} = \frac{1}{L} \int_0^L \frac{1}{2} \rho g \zeta^2 dx. \quad (5.2)$$

Use of Equations (3.10) and (3.11) gives us, to second order,

$$\text{K.E.} \approx \frac{\rho g}{4} \sum_k \frac{1}{k^2} \left[b_k^{(+)} + b_k^{(-)} \right] \left[b_{-k}^{(+)} + b_{-k}^{(-)} \right], \quad (5.3)$$

and

$$\text{P.E.} = - \frac{\rho g}{4} \sum_k \frac{1}{k^2} \left[b_k^{(+)} - b_k^{(-)} \right] \left[b_{-k}^{(+)} + b_{-k}^{(-)} \right]. \quad (5.4)$$

Here we have also made the approximation of replacing G_k by g in Equation (3.10). The distinction between G_k and g is important only for the shorter wavelengths, which are expected to contribute relatively little to the energy and also to violate the expansion in Equation (3.17).

For right-travelling waves only, the energy is just

$$\text{K.E.} + \text{P.E.} = \frac{\rho g}{2} \sum_{k>0} \frac{|q_k^{(+)}|^2}{k^2}. \quad (5.5)$$

The surface contour obtained from the definition of the mode expansion [Equation (2.14)], is,

$$\zeta(x,t) = - \sum_k \frac{1}{|k|} \operatorname{Im} \left\{ q_k^{(+)} e^{i[kx - \omega_k t]} \right\} \quad (5.6)$$

for waves travelling only to the right, we keep only terms with $k > 0$, here. For the case of a single mode, Equation (5.6) reduces to Equation (3.16), of course.

We wish to write Equation (5.6) so as to remove the primary wave component from the oscillation. To do this we write the primary wave number $k = k_0$ so that,

$$\begin{aligned} \omega_k &= \sqrt{g(k_0 + \kappa)} \approx \omega_{k_0} \left\{ 1 + \frac{1}{2} \frac{\kappa}{k_0} + \dots \right\} \\ &= \omega_{k_0} + \kappa v_G \end{aligned} \quad (5.7)$$

where the group velocity (v_G) of the primary wave is given by $\frac{1}{2} \omega_{k_0}/k_0$. The wave envelope can, therefore, be written as,

$$\zeta(x,t) = - \sum_k \frac{1}{|k|} \operatorname{Im} \left\{ q_k^{(+)} e^{i[k_0 x - \omega_0 t]} e^{i\kappa[x - v_G t]} \right\} \quad (5.8)$$

Alternatively we can express Equation (5.8) in terms of a phase and amplitude modulation by defining the quantities

$$G = G_R + i G_I = \sum_k q_k^{(+)} e^{i\kappa(x - v_G t)} \quad (5.9)$$

and

$$\theta_0 = k_0 x - \omega_0 t \quad . \quad (5.10)$$

Substituting Equations (5.9) and (5.10) into (5.8) yields

$$\zeta(x, t) = \sqrt{G_R^2 + G_I^2} \left\{ \frac{G_I}{|G|} \cos \theta_0 + \frac{G_R}{|G|} \sin \theta_0 \right\} \quad (5.11)$$

or

$$\zeta(x, t) = |G| \cos \left[\theta_0 - \arctan \left(\frac{G_R}{G_I} \right) \right] \quad . \quad (5.12)$$

The modulation of the surface waves, i.e., the surface envelope is therefore given by the function,

$$|G| = \left| \sum_k q_k^{(+)} e^{i\kappa(x - v_G t)} \right| \quad . \quad (5.13)$$

6. SAMPLE CALCULATION AND CONCLUSION

The purpose of doing a sample calculation is twofold: (i) to test the numerical methods in a simple case which can be compared to an analytic calculation, and (ii) to determine instructive ways of presenting the results of the calculation. For our test calculation we have selected what we feel to be the simplest problem which is still of some physical interest. The initial state in the test problem consists of three equally spaced non-zero modes, the center mode being an order of magnitude larger in amplitude than its side bands. The interaction between the modes is described by Equation (3.24) and the growth of all the modes in the system is calculated.

This problem is the one considered both experimentally and theoretically (linear) by Benjamin and Feir (1967) and which lead them to the conclusion that a Stokes wave is unstable. The experiment consisted of generating a mechanical wave of fairly large slope (0.17) in a wave tank and modulating this wave with two low amplitude waves (perturbations) at the side bands of the primary wavenumber. These perturbations were found to grow exponentially from out of the background noise on the tank surface and eventually caused the primary wave to break up. The details of this break-up process will be discussed below in terms of the present calculation.

We have limited the total number of modes in this first calculation to nine. This number is somewhat arbitrary but it is large enough to indicate the general behavior of the system when the number of modes is increased. Comparisons with the results from a second calculation with thirteen modes is also made. Also, the present number of modes does yield accurate quantitative results over a time scale long compared to the characteristic growth time of each of the separate modes.

The wavenumbers for our modes are chosen such that,

$$k = \frac{2\pi}{L} \kappa ; \quad \kappa = 0, 1, 2, \dots, N \quad (6.1)$$

where L is a length representing the region of interest of the ocean surface and κ is an integer. Because we wish to make some comments on the comparison of the present calculation and the experiment of Benjamin and Feir, we select a length ($L = 2.1946 \times 10^4$ cm) and integer ($\kappa = 100$) such that the central wave-number (k) is that of the primary wave in their experiment, i.e., $k = 0.02863 \text{ cm}^{-1}$. Our first calculation will not use the experimental amplitudes since these values lead to a very rapid break up of the primary wave. The initial configuration is shown in Figure 3 labeled "time = 0 sec." We have selected an initial amplitude of the primary mode to be $|q_k^{(+)}| = 0.071$ and $|q_{k\pm 1}^{(+)}| = 0.014$ for the secondary modes which corresponds to wave amplitudes of 2.46 cm for the primary and 0.45 cm for the greater and 0.55 cm for the lesser of the secondary modes. The remainder of the nine mode amplitudes are initially zero.

The results of this calculation are presented in Figures 3 through 6. In Figure 3, we show a series of snapshots of the modulus of the mode slopes. Each snapshot indicates how the energy has redistributed itself between the modes from the preceding snapshot. We can see that the energy of the system which at time zero was concentrated in the three central modes diffuses outward into the neighboring modes of the system in time. Those modes closer to the central mode grow faster than the more distant modes. It is evident from Figure 3 that the evolution of the modes closely resembles the process of diffusion. This notion of the diffusion of energy between modes due to non-linear interactions will be explored more fully in a subsequent report (PD-72-029) which models the interaction process between ocean waves in terms of a transport equation.

In Figure 4 the sensitivity of the preceding calculation to changes in mode number is shown. Maintaining the spacing between modes we increase the width of our k-space interval by four modes maintaining the same central mode. It is clear that these additional modes have no effect on the growth for $t \leq 80$ sec since only the 12th mode has significant amplitude up to this time.

Figure 5 is a continuous representation of the information in Figure 3, showing how each of the mode amplitudes grow as a function of time. We can see from Figure 3 that

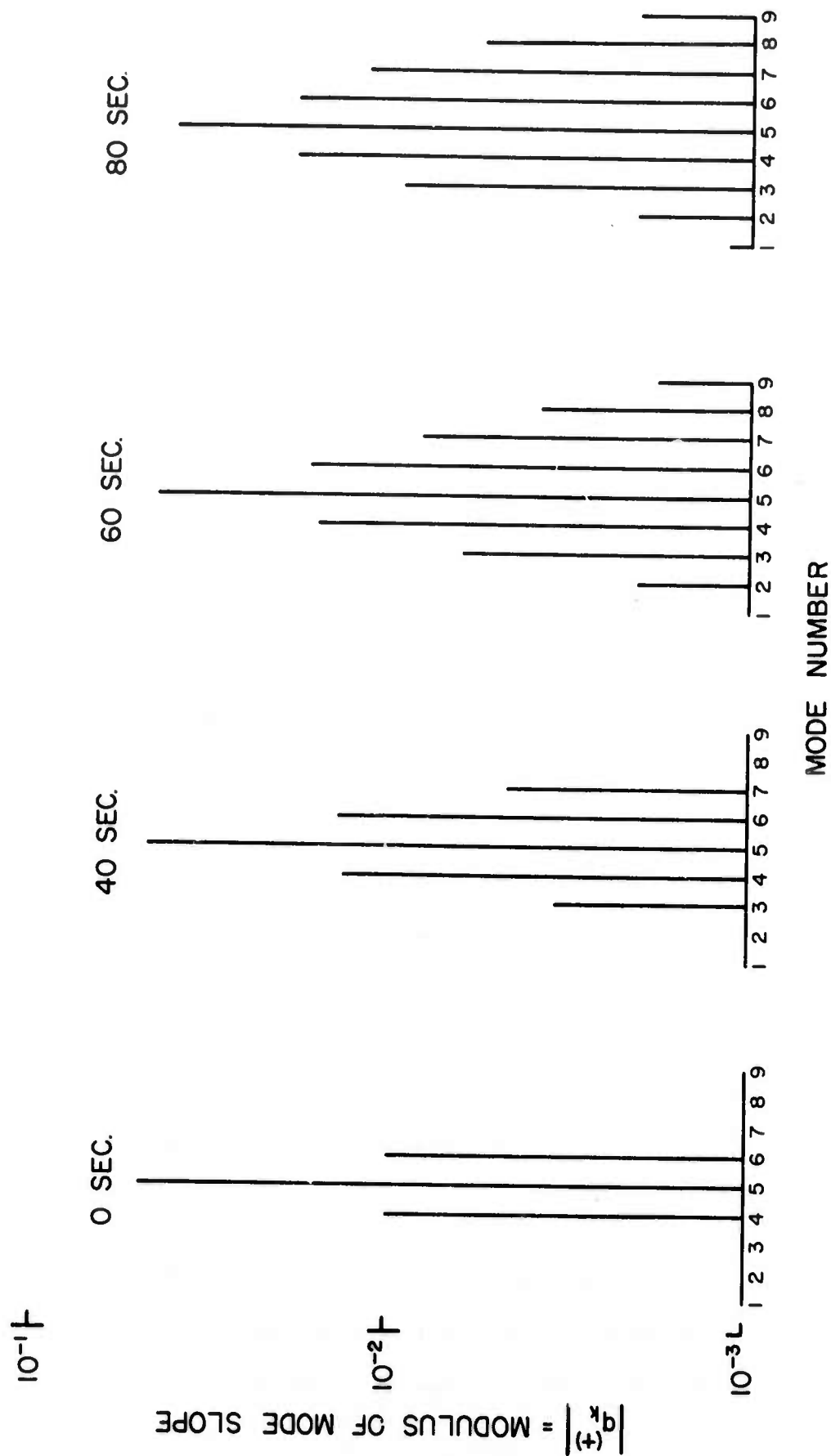
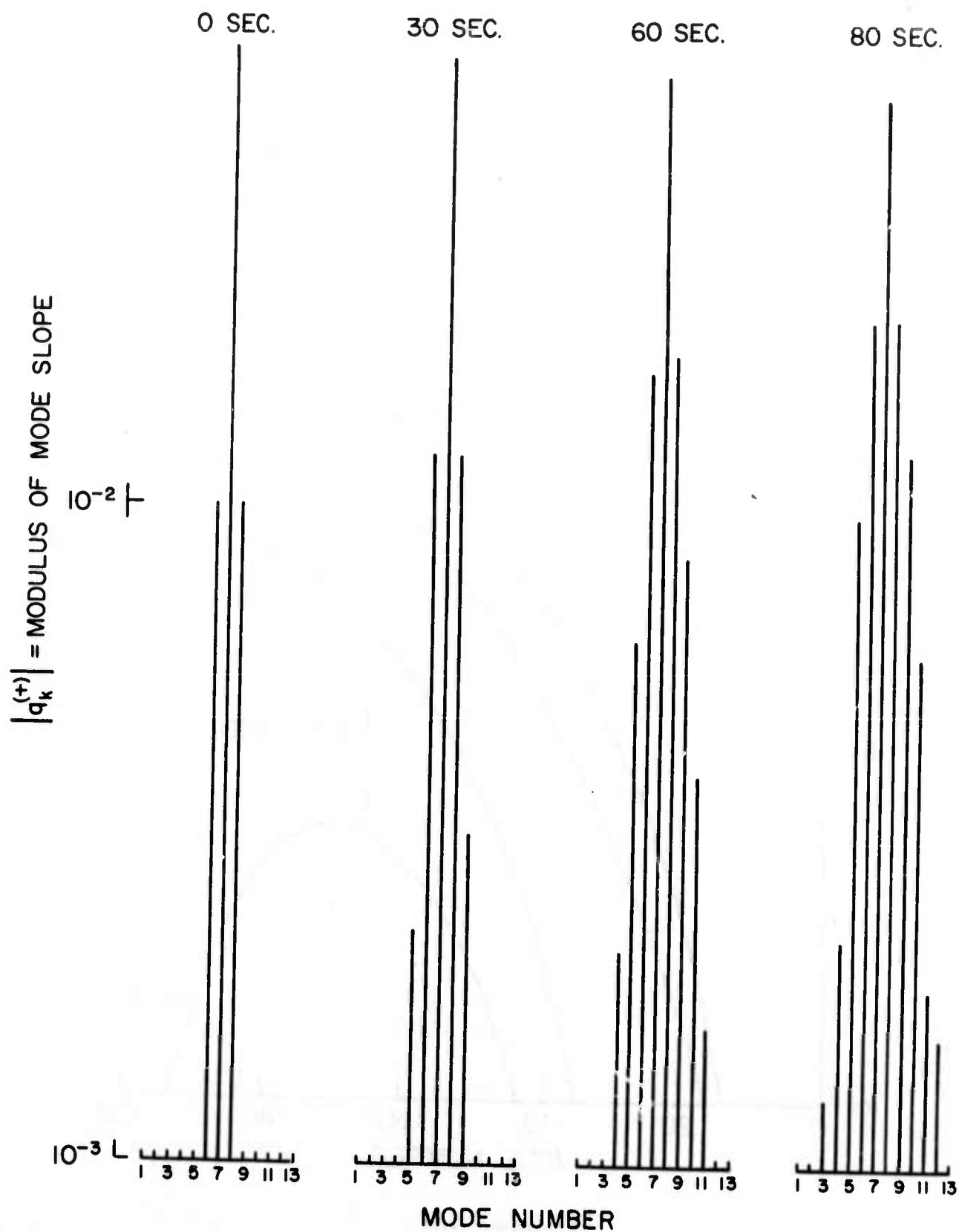


FIGURE (3)

10^{-1} Γ

FIGURE (4)



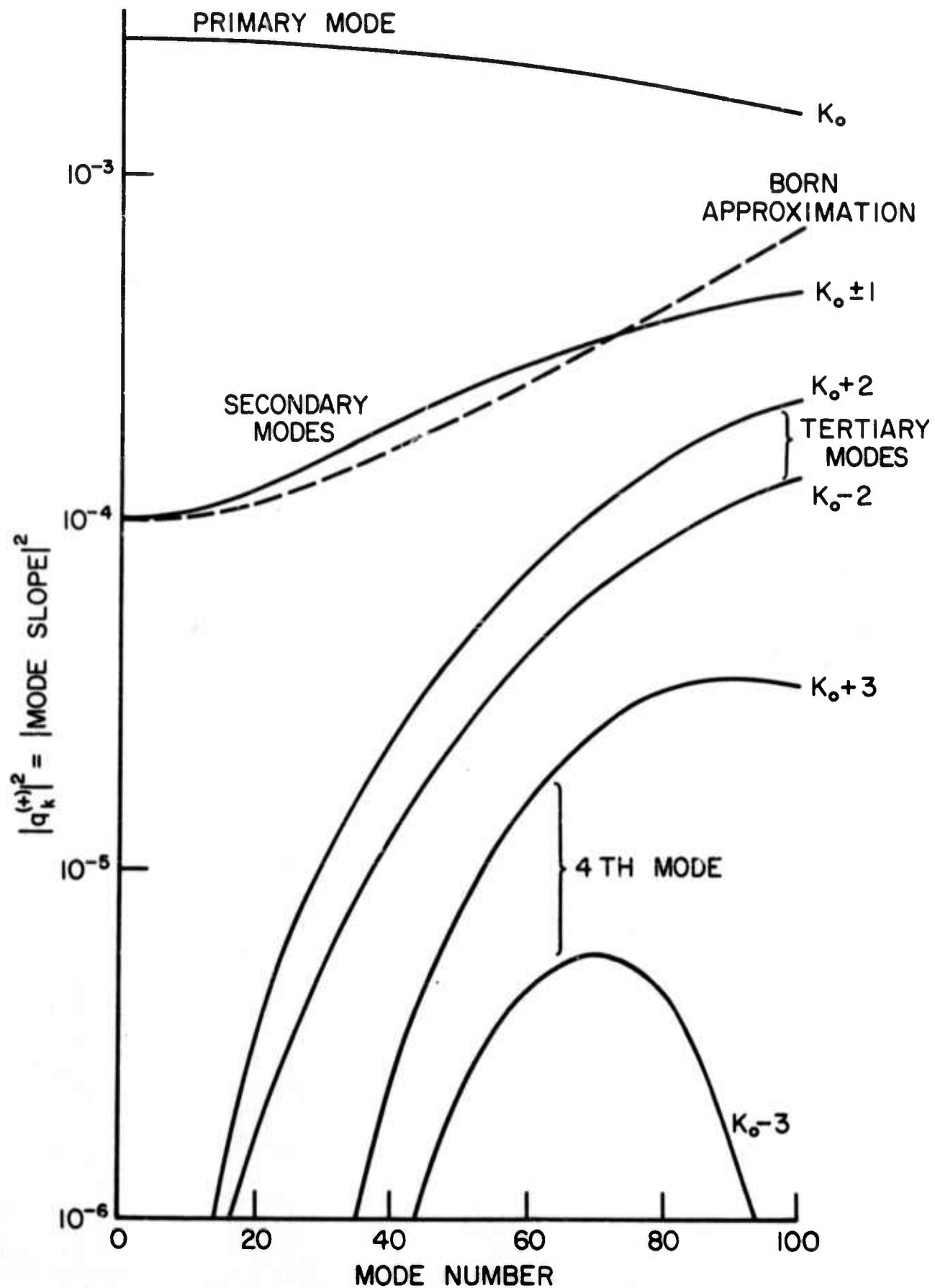


FIGURE (5)

the side bands do not grow at exactly the same rate, but close enough that a single line may be used in Figure 5 to represent the growth of both these modes. The central mode ($\kappa_0 = 100$) is labeled "Primary Mode" in Figure 5, the first side bands ($\kappa = 99$ and 101) are labeled "Secondary Mode," etc. In this figure we compare our calculations to an analytic result, i.e., the Born approximation. The Born approximation for this problem is calculated by assuming, (i) that the amplitude of the primary mode is constant throughout the interaction process, and (ii) the frequencies of the primary and secondary modes are approximately equal. The interaction equations then become,

$$\dot{q}_{\kappa_0+1} \approx -\frac{i\omega_{\kappa_0}}{2} \left[|q_{\kappa_0}|^2 q_{\kappa_0+1} + q_{\kappa_0}^2 q_{\kappa_0-1}^* \right] , \quad (6.2)$$

$$\dot{q}_{\kappa_0} \approx 0 \quad (6.3)$$

and

$$\dot{q}_{\kappa_0-1} \approx -\frac{i\omega_{\kappa_0}}{2} \left[|q_{\kappa_0}|^2 q_{\kappa_0-1} + q_{\kappa_0}^2 q_{\kappa_0+1}^* \right] \quad (6.4)$$

since, by assumption (ii)

$$\omega_{\kappa_0} \approx \omega_{\kappa_0+1} \approx \omega_{\kappa_0-1} \approx \sqrt{\frac{2\pi}{L}} g \kappa_0 . \quad (6.5)$$

We may use Equations (6.2) - (6.4) to construct the equation

$$\frac{d}{dt} |q_{\kappa_0+1}|^2 = \frac{d}{dt} |q_{\kappa_0-1}|^2 = -\omega_{\kappa_0} q_{\kappa_0}^2 \text{Im} \{ q_{\kappa_0+1} q_{\kappa_0-1} \} \quad (6.6)$$

where $\text{Im}\{\}$ refers to the imaginary part of the bracketed quantity. Since our initial conditions are $q_{\kappa_0+1}(0) = q_{\kappa_0-1}(0) = q$ and $q_{\kappa_0}(0) = q_{\kappa_0}^*(0)$, Equation (6.6) has the solution

$$q_{k_0+1}(t) = q_{k_0-1}(t) = q \left\{ \cosh \left[\omega_{k_0} |q_{k_0}|^2 \frac{t}{2} \right] - i \sinh \left[\omega_{k_0} |q_{k_0}|^2 \frac{t}{2} \right] \right\} . \quad (6.7)$$

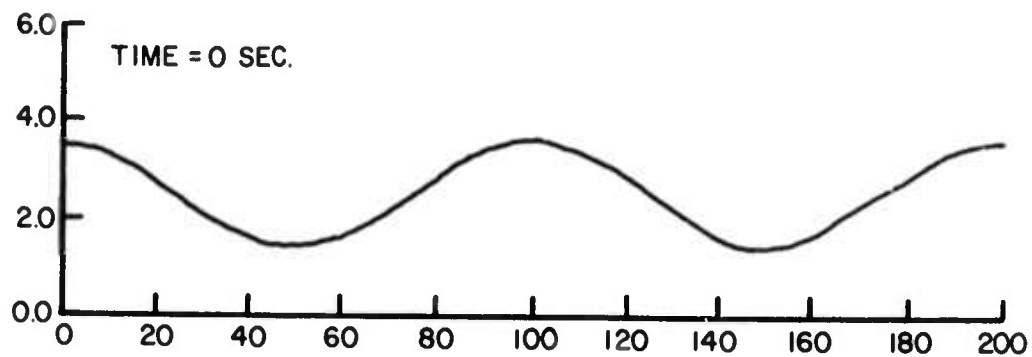
The Born approximation to the secondary modes plotted in Figure 5 is, therefore,

$$|q_{k_0+1}|^2 = |q_{k_0-1}|^2 = q^2 \cosh \left[\omega_{k_0} |q_{k_0}|^2 t \right] . \quad (6.8)$$

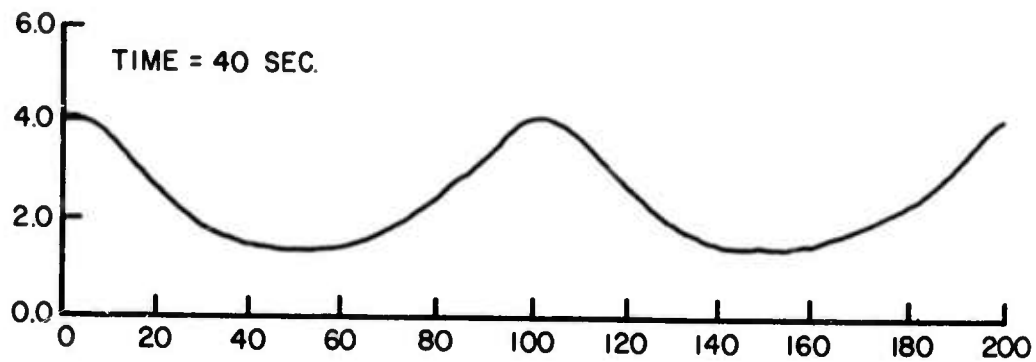
We see that the growth of the secondary mode is similar to Equation (6.8) in the region where the approximations made are nearly valid, that is, for a near constant primary mode. The development is markedly different, however, after the higher modes have grown to an appreciable size, that is, the secondary modes cease growing and begin losing their energy. The energy is depleted from the secondary and primary modes, causing the growth of the more central modes to be inhibited. It is not shown here, but the energy drain of the primary mode does not persist, it begins growing after the other modes of the system are of the same order of magnitude. The detailed manner of this growth has yet to be explored.

In Figure 6 we illustrate the envelope of the surface waves in a region of ocean 438 meters long. The envelope is calculated as it travels with the group velocity of the primary wave (9.26 m/sec) so that each envelope shown, i.e., different time snapshots, is constructed from the same group of waves as they propagate along the ocean surface. In Figure 6a

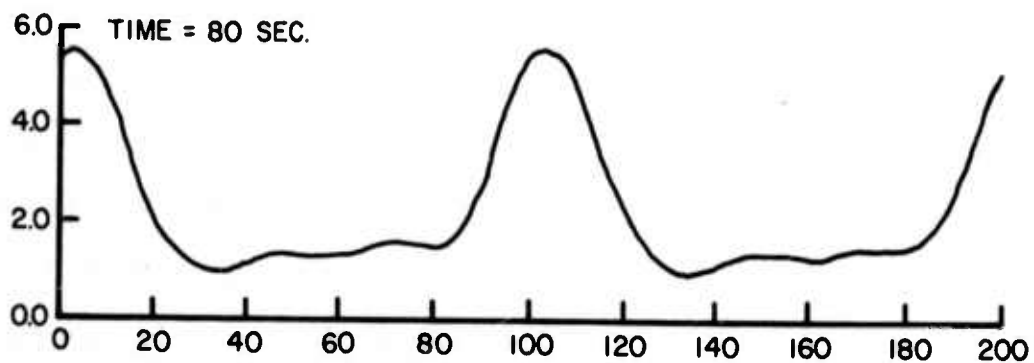
AMPLITUDE OF SURFACE ENVELOPE



(6A)



(6B)



DISTANCE IN UNITS OF λ_{primary} (= 2.194 meters)

(6c)

FIGURE (6)

we see that (time $t=0$) the modulation of the ocean surface is slow, but significant over the region of interest. This is due to the large initial amplitude of the secondary modes. The step size is given in units of the primary wavelength, i.e., $\lambda = 2.194$ meters. The initial undulation of the envelope seems to be compressed in time into a series of bumps. These bumps rapidly become accentuated, forming wave packets on the surface. It will be seen, however, that the large structure in Figure 6 is due to the periodic boundary conditions imposed on the problem and does not represent the breakup seen experimentally by Benjamin and Feir.

The significant structure in Figure 6 lies between the modulation peaks. In this region the modulation remains fairly constant during the time in which energy is diffusing out of the center mode (see Figures 3 and 4). As the amplitude of the higher modes increases, however, the structure of the wave envelope changes. The extreme case is shown in Figure 6c where the detailed modulation of the surface waves has clearly developed. It is difficult to determine the surface structure by looking at only a picture of the modulation so we introduce a parameter to indicate the degree of distortion.

To characterize the distortion of the ocean surface, we use the ratio of the difference between the maximum and mini-

mum envelope height to the average envelope height. In Figure 7 we use this quantity to indicate the growth in the surface wave amplitude modulation. The solid curve refers to the sample calculation above, the dashed to a simulation of the Benjamin-Feir experiment. We see in Figure 7 that for $t \leq 70$ sec, essentially no change is observed in the modulation of the surface. Note that we have removed the effects of the large bumps in Figure 6 and are concerned only with the "actual" modulation which lies between the bumps. The sudden growth of the surface distortion ($t \geq 70$ sec) occurs when the magnitude of the modes becomes comparable (see Figures 3 and 4) so that large transfers of energy can take place in small interaction times.

The second curve in Figure 7 represents the growth of the surface distortion from the calculation using the initial conditions of the B-F experiment. This calculation again uses nine modes, with the central mode corresponding to the mechanically generated wave. The experimental conditions were simulated by giving each of the remaining modes the uniformly small value of 0.001, which is intended to reproduce the noise at the tank surface. In terms of our variable, the central mode amplitude is $q_{MID}^{(+)} = 0.17$ corresponding to a primary wave of 5.93 cm amplitude. These initial conditions are shown by the "time = 0" graph in Figure 8.

FIGURE (7)

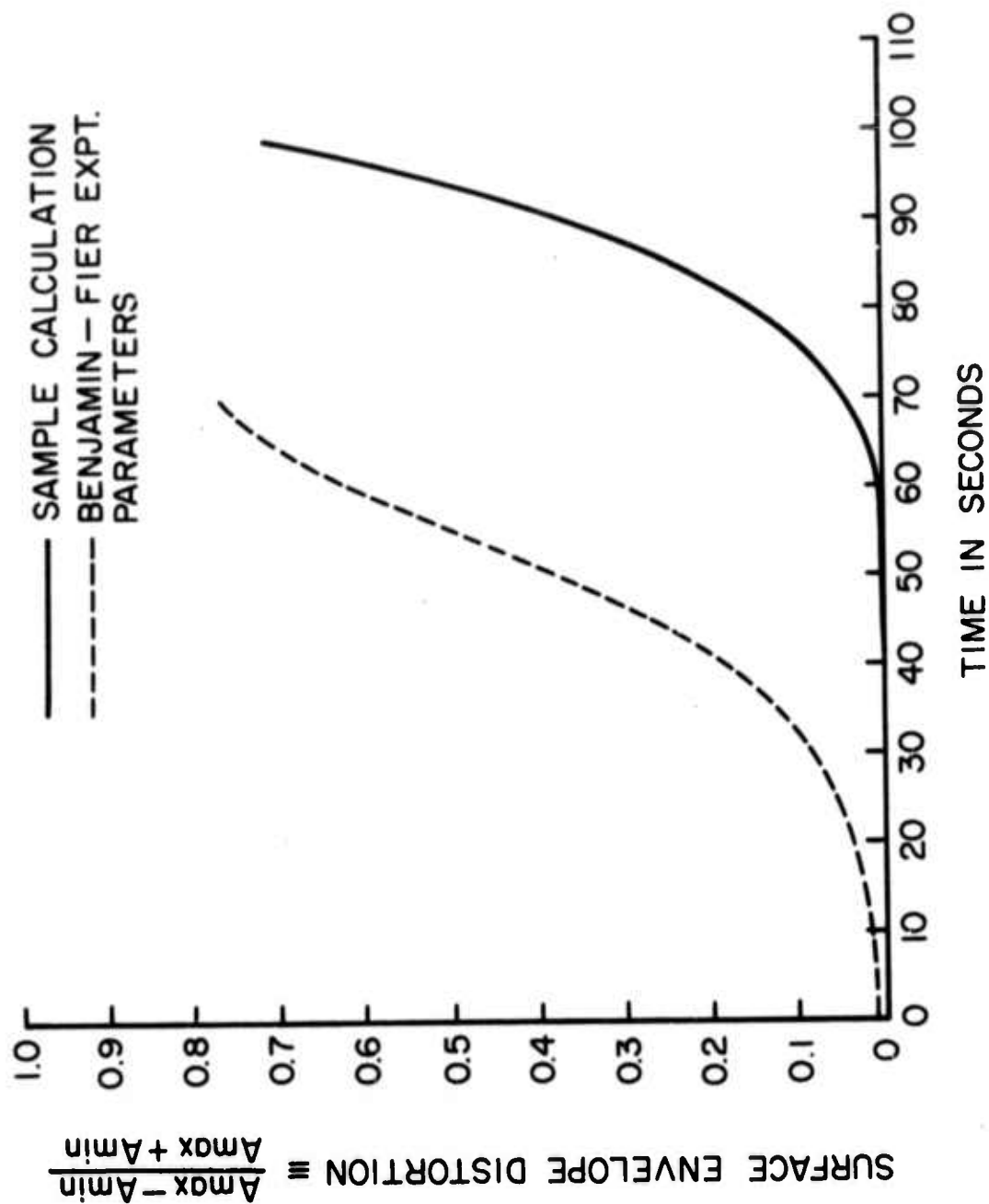


FIGURE (8)

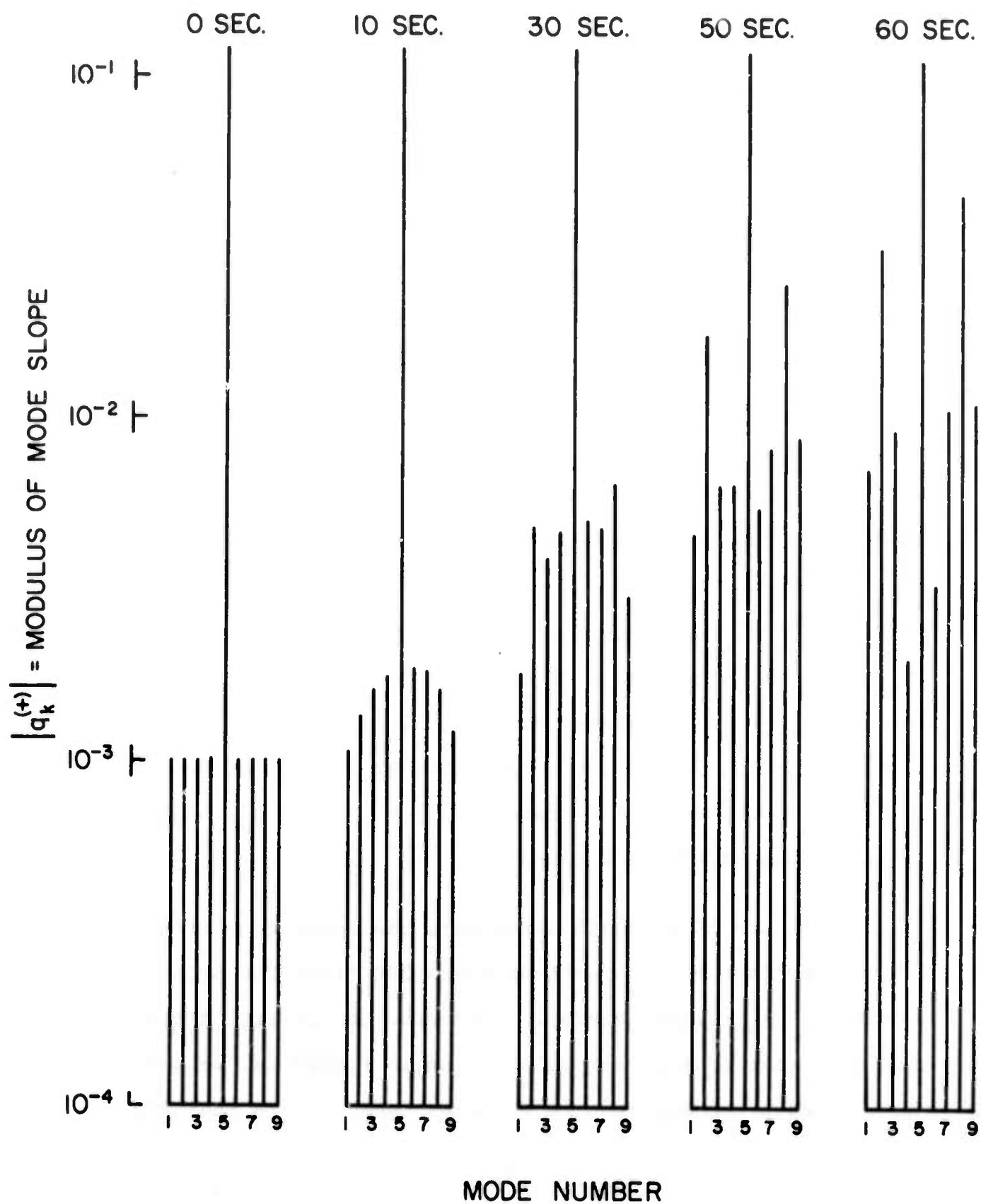
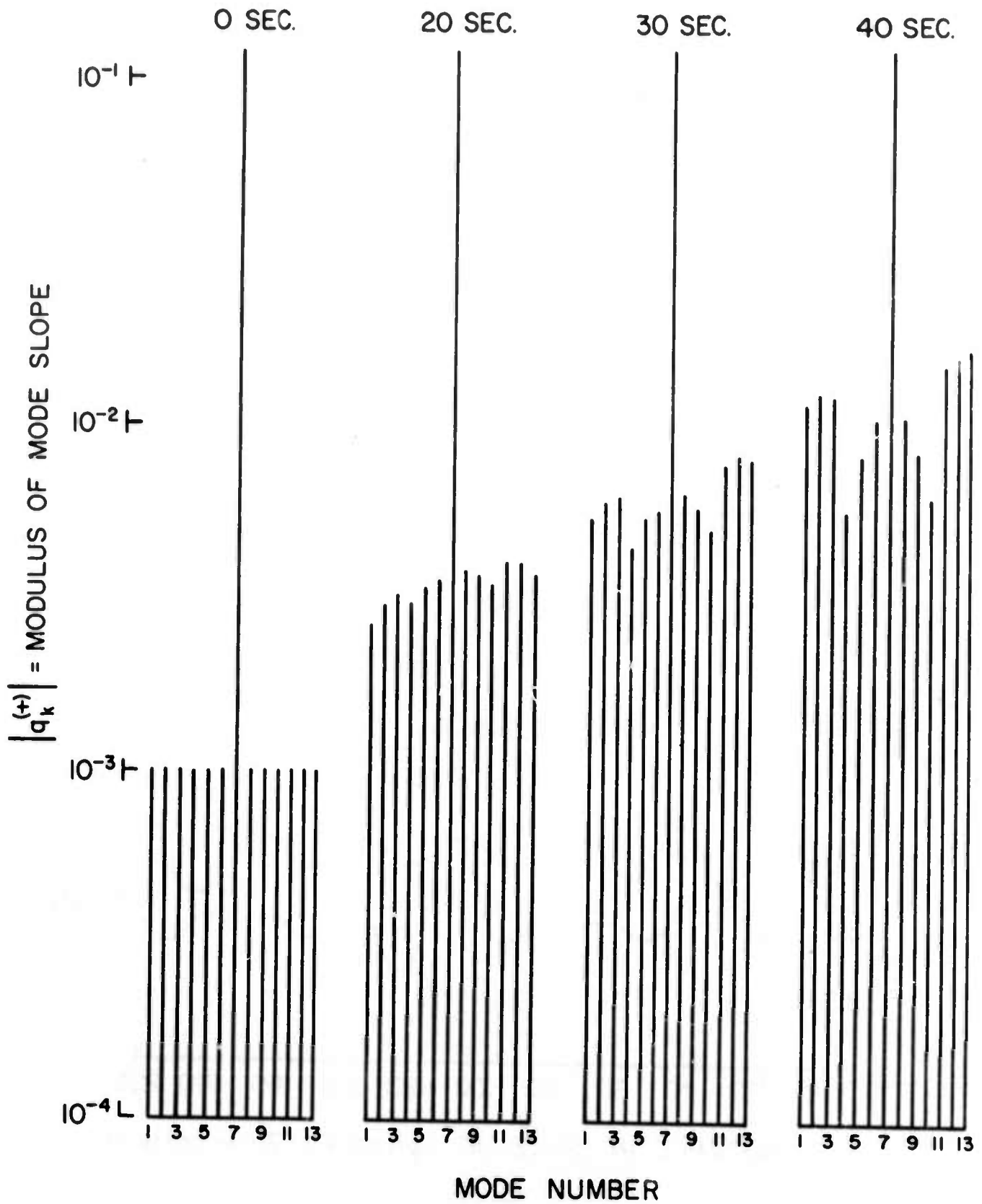
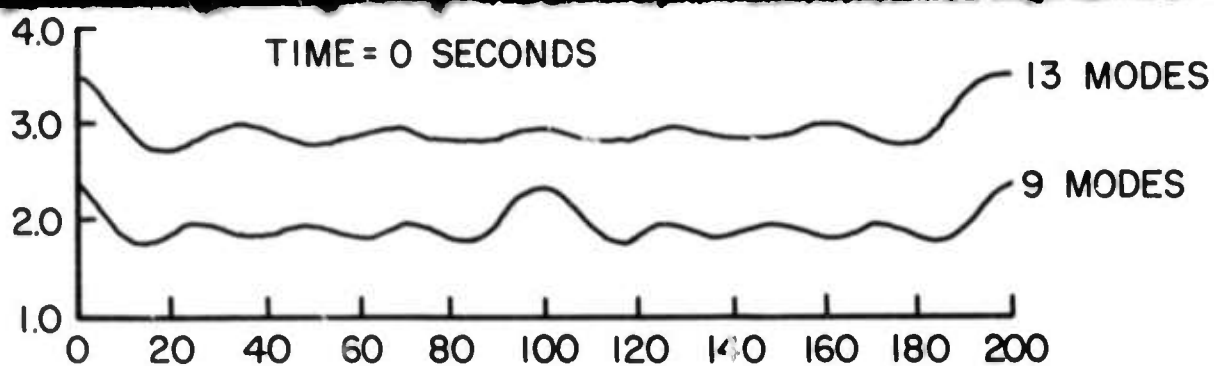


Figure 8 depicts the modulus of the mode amplitude at different instants of time just as Figure 3 for the test calculation. We can see that the non-linear interactions preferentially amplify the side bands which differ from the primary by $\pm 3\Delta k$, where Δk is the step size in wavenumber space. These side bands are 1.3 and 0.7 of the central wavenumber (κ_0). This is in essential agreement with the perturbation analysis of Benjamin which shows that the frequency side bands at 1.1 and 0.9 of ω_0 would be preferentially amplified from out of the background noise. The effect of increasing the number of modes in this calculation is shown in Figure 9, where we have reduced the step size Δk by a factor of two. In Figure 9 the mode numbers which differ from the primary by $\pm 10\%$ are modes 1 and 13. We can see that instead of a single mode on each side of the primary being preferentially amplified we have a preferred group of modes being amplified. This would seem to indicate the validity of the preferred mode concept in the continuous limit, where a group of waves in a region $\delta\omega$ about the average position $\pm 10\%$ of ω_0 would be picked out of the background.

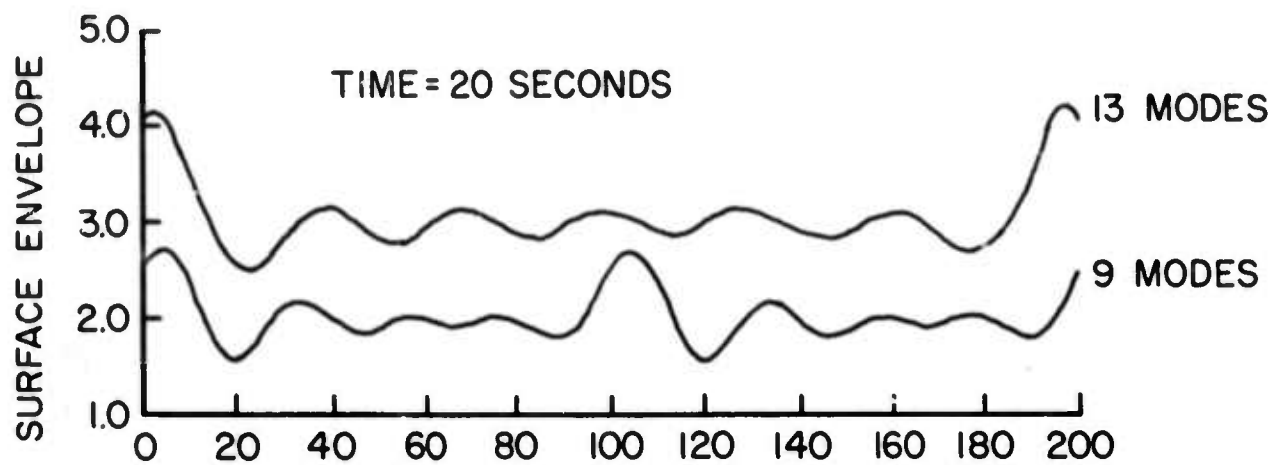
In Figure 10 we again illustrate the modulation of the surface envelope on a stretch of ocean 200 times the primary wavelength ($\lambda_p = 2.194$ meters). Comparing the initial distortion with that of the test calculation in Figure 6a, we see that the direct comparison is somewhat deceptive in that the

FIGURE (9)

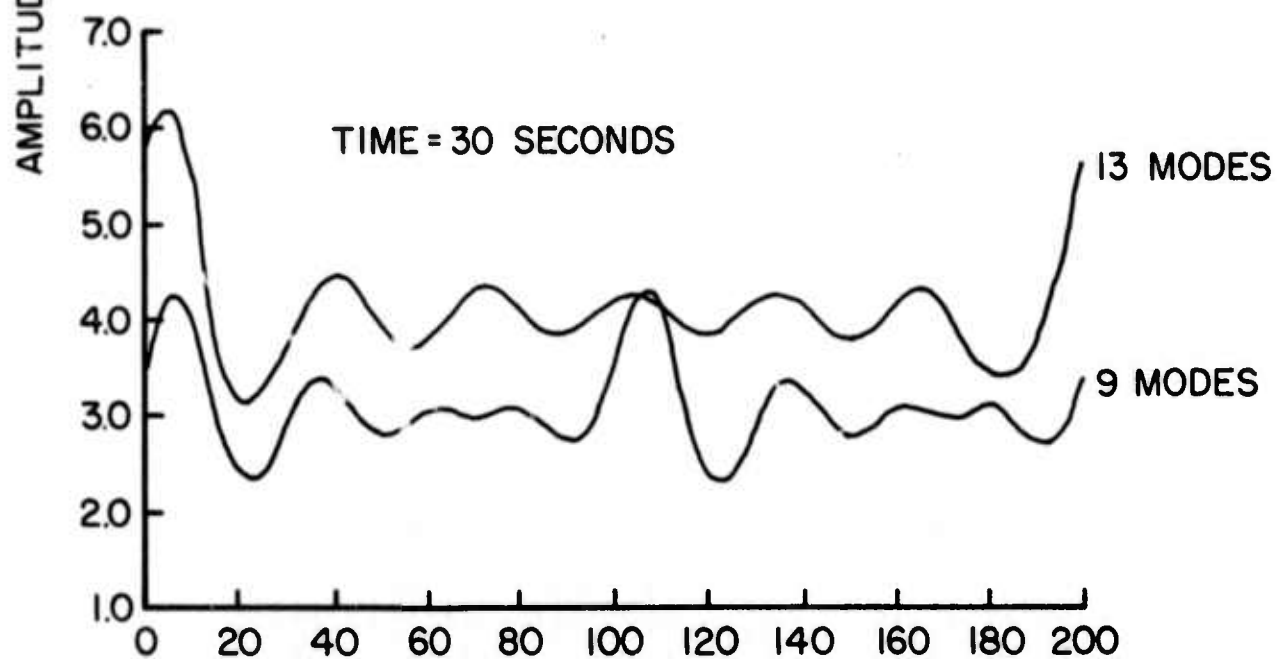




(10A)



(10B)



DISTANCE IN UNITS OF λ_{primary} (= 2.194 meters)

(10c)

FIGURE (10)

B-F case has a greater initial distortion which is not evident from the figure. In Figure 10 the surface modulation for both the 9 and 13 mode B-F cases discussed are given. We see that the effect of decreasing the mesh size by a factor of two in k-space has displaced the central bump in the 9 mode calculation from $100 \lambda_p$ to $200 \lambda_p$ in the 13 mode calculation. The effect of this reduction is most clearly seen in the "time = 30" graph. Although the 9 mode calculation does show the modulation of the surface waves, the envelope becomes distorted as it approaches the $1/\Delta k = 100\lambda_p$ point in the figure, i.e., the periodic boundary. This effect is markedly reduced in the 13 mode calculation which shows precisely the type of surface modulation observed by Benjamin and Feir. This comparison indicates that caution must be exercised in the selection of the mode spacing used in a particular calculation. The amplitude scales in Figure 10 are arbitrary because the 9 and 13 mode curves were shifted so as to provide the best visual comparison. The initial curves are actually superimposed.

The distance the primary wave travelled in the B-F experiment prior to breaking up was approximately twenty-eight wavelengths. The corresponding time interval is 33 seconds. We see from Figure 10 that the distortion of surface becomes quite significant ($\approx 10\%$) at this time, which agrees well with the experiment.

It is clear that when the primary wave initially contains most of the energy in the wave system, that the coherent non-linear interactions between the surface gravity waves lead to a breakup of this wave into packets. The characteristic time for this breakup is determined by the details of the initial conditions. The breakup is seen as a distortion of the surface envelope. This distorting occurs as energy coherently diffuses from the primary to the other modes in the system. As additional modes develop the surface distortion increases markedly, but the pattern of the distortion does not change. We see this in Figure 10 where the initial pattern in the B-F experiment translates and grows but does not change in shape. This would indicate that the group velocity of the pattern, which is that of the primary wave, changes only slightly as the other modes develop; also that the phases of the other modes "lock" onto that of the primary so as to create the stationary pattern.

If such an effect were present on the real ocean it could be observed with radar. The radar return from such a surface would indicate the envelope structure and "see" the phase-locking effect. The distorted envelope would yield a strong correlation centered at the frequency of the primary wave.

APPENDIX A

To integrate Eq. (3.29) over the interval $0 \leq t \leq T$, we choose a time step Δ , where T/Δ is an integer. Let

$$t_j = j\Delta, \quad j = 0, 1, 2, \dots, T/\Delta.$$

Integration of Eq. (3.29) over the interval t_j to t_{j+1} is done in the form:

$$q_k^{(+)}(t_j + \Delta) = \left[1 + \left(\frac{\alpha k |k|}{2 \omega_k} - v k^2 \right) \Delta \right] q_k^{(+)}(t_j) + i \sum_{\ell+p=k+n} \Gamma_{\ell pn; k} I_{\ell pn; k}(j), \quad (A.1)$$

where

$$I_{\ell pn; k}(j) \equiv \int_{t_j}^{t_{j+\Delta}} H_{\ell pn} e^{i\Omega_{\ell pn k} t} dt. \quad (A.2)$$

The numerical evaluation of Eq. (A.2) is done as follows:

Write [we drop for the moment the (ℓ, p, n, k) subscripts]

$$H(t) \equiv H_m(t) e^{i\phi(t)}, \quad (A.3)$$

where H_m and ϕ are real. We suppose for the evaluation of $I(j)$

the $q_k^{(+)}(t_j)$ and $q_k^{(+)}(t_j - \Delta)$ are stored. We can thus evaluate

$$H_0 \equiv H_m(t_j + \frac{\Delta}{2}) \cong H_m(t_j) + \frac{\Delta}{2} H_1 ,$$

$$H_1 = [H_m(t_j) - H_m(t_j - \Delta)]/\Delta , \quad (A.4)$$

and

$$\phi_0 \equiv \phi(t_j + \frac{\Delta}{2}) \cong \phi(t_j) + \frac{\Delta}{2} \phi_1 ,$$

$$\phi_1 = [\phi(t_j) - \phi(t_j - \Delta)]/\Delta . \quad (A.5)$$

We may then express $I(j)$ [Eq. (A.2)]

$$\begin{aligned} I(j) &\cong e^{i[\Omega(t_j + \frac{\Delta}{2}) + \phi_0]} \\ &\times \int_{-\frac{\Delta}{2}}^{\frac{\Delta}{2}} [H_0 + H_1 \tau] e^{i[\Omega + \phi_1]\tau} d\tau \\ &= e^{i[\Omega(t_j + \frac{\Delta}{2}) + \phi_0]} [H_0 L_0 + H_1 L_1] , \end{aligned} \quad (A.6)$$

where

$$\begin{aligned} L_0 &= \frac{2}{(\Omega + \phi_1)} \sin [(\Omega + \phi_1)\Delta/2] , \\ L_1 &= \frac{i}{(\Omega + \phi_1)^2} \left\{ 2 \sin [(\Omega + \phi_1)\Delta/2] \right. \\ &\quad \left. - ((\Omega + \phi_1)\Delta) \cos [(\Omega + \phi_1)\Delta/2] \right\} . \end{aligned} \quad (A.7)$$

In Equation (A.6) we have introduced the new variable of integration $\tau = t - (t_j + \Delta/2)$.

To check the numerical accuracy of the calculation at each step of the integration the energy is calculated using Equation (5.5). Since the energy will be conserved in the absence of wind and viscosity, this provides a quantitative check of our procedure.

REFERENCES

- Benjamin, T. B., (1967), Royal Soc. of London, Proceedings,
A299, 59.
- Benjamin, T.B. and J. E. Feir, (1967), J. Fluid Mech. 27, 417.
- Cohen, B. I., A. N. Kaufman and K. M. Watson, (1971), Phys.
Rev. Lett. 29, 581.
- Hasselmann, K., (1961), J. Fluid Mech. 12, 481.
- Hasselmann, K., (1966), Reviews of Geophysics 4, 1.
- Phillips, O. M., (1966), The Dynamics of the Upper Ocean,
Cambridge University Press.
- Whitham, G. B., (1966), Royal Soc. of London, Proceedings, V299.